Environmental Chemistry Letters (2021) 19:441–463
https://doi.org/10.1007/s10311-020-01077-8

REVIEW

Photocatalysis for removal of environmental pollutants and fuel production: a review

Anbalagan Saravanan[1] · Ponnusamy Senthil Kumar[2] · Dai-Viet N. Vo[3] · Ponnambalam Ragini Yaashikaa[2] · Suresh Karishma[1] · Sathasivam Jeevanantham[1] · B. Gayathri[1] · V. Dhivya Bharathi[1]

Received: 28 July 2020 / Accepted: 13 August 2020 / Published online: 27 August 2020
© Springer Nature Switzerland AG 2020

Abstract

Water pollution and fossil fuels are major issues in the context of climate change. Photocatalysis research is rising to develop green technologies for the remediation of pollutants and for energy production. Photocatalysis converts the light energy as photons into chemical energy using semiconducting materials. Different methods are utilised to synthesise these photocatalytic materials. Metal and coupled metal frameworks are applied for the production of photocatalytic materials. Here we review the synthesis and applications of photocatalysts for environmental decontamination and for production of biodiesel, methanol and hydrogen. Pollutants include dyes, pesticides, herbicides, phenols and antibiotics.

Keywords Photocatalytic removal · Environmental pollutants · Degradation mechanism · Novel photocatalysts · Fuel production

Abbreviations

3D Fe_2O_3	Three-dimensional ferric oxide
As(V)	Arsenate
Cr(VI)	Hexavalent chromium
$Na_2HAsO_4{\cdot}7H_2O$	Disodium hydrogen arsenate heptahydrate
$K_2Cr_2O_7$	Potassium dichromate
PAEC	Plasma atomic emission spectroscopy
Fe_2O_3	Ferric oxide
TiO_2	Titanium dioxide
ZnO	Zinc oxide
$CuCo_2S_4$	Copper cobalt sulphide
$MoSe_2/BiVo_4$	Molybdenum diselenide/bismuth vanadate
$Bi(NO_3)_3.H_2O$	Bismuth(III) nitrate monohydrate
NH_4VO_3	Ammonium metavanadate
CO_2	Carbon dioxide
Cu^{2+}	Copper(II) ion
Zn^{2+}	Zinc(II) ion
Ni^{2+}	Nickel(II) ion
Pb^{2+}	Lead(II) ion
$Cu(NO_3){\cdot}3H_2O$	Copper(II) nitrate trihydrate
$Zn(NO_3)_2{\cdot}6H_2O$	Zinc nitrate hexahydrate
$Ni(NO_3)_2{\cdot}6H_2O$	Nickel(II) nitrate hexahydrate
$Pb(NO_3)_2$	Lead(II) nitrate
pH	Potential of hydrogen
HNO_3	Nitric acid
Rh–Sb TiO_2	Rhodium and antimony co-doped titanium dioxide
RS-TONR/TNT	Rhodium/antimony co-doped titanium oxide nanorod and titanate nanotube
Cr(III)	Trivalent chromium
$Bi(NO_3)_3$	Bismuth(III) nitrate
Na_2WO_4	Sodium tungstate
$AgIn_5S_8$	Silver indium sulphide
Bi_2WO_6	Bismuth tungstate
FeS_2	Iron disulphide
BiOCl–Ag–AgBr	Bismuth oxychloride silver bromide
BiOCl	Bismuth oxychloride
$NaFeS_2$	Sodium iron disulphide

✉ Ponnusamy Senthil Kumar
senthilchem8582@gmail.com; senthilkumarp@ssn.edu.in

[1] Department of Biotechnology, Rajalakshmi Engineering College, Chennai 602105, India

[2] Department of Chemical Engineering, Sri Sivasubramaniya Nadar College of Engineering, Chennai 603110, India

[3] Center of Excellence for Green Energy and Environmental Nanomaterials (CE@GrEEN), Nguyen Tat Thanh University, Ho Chi Minh City, Vietnam

$NaNO_3$	Sodium nitrate
TiO_2 QD	Titanium oxide quantum dots
Cu_2O NPs	Copper oxide nanoparticles
Cu_2O	Cuprous oxide
$Cu(NO_3)$	Copper(I) nitrate
TiO_2/MoS_2	Titanium oxide molybdenum sulphide
$TiCl_4$	Titanium tetrachloride
MoS_2	Molybdenum sulphide
Sm@POA–TP	Samarium codoped poly o-anisidine titanium phosphate
POA–TP	Poly o-anisidine titanium phosphate
H_2O_2	Hydrogen peroxide
ZnS	Zinc sulphide
CTAB	Cetyl trimethyl ammonium bromide
NH_3OH	Ammonium hydroxide
MCM-41	Mobil composition of matter 41
$Co(NO_3)_2{\cdot}H_2O$	Cobaltous nitrate hexahydrate
HPLC	High pressure liquid chromatography
Co_3O_4/SF–MCM-41	Cobalt tetraoxide silica fume Mobile composition of matter 41
TNP–Pd–Fe_3O_4/GO	Titanium nanoplate palladium-doped ferric oxide graphene oxide
Fe_3O_4	Ferrosoferric oxide
SO_4^{2-}	Sulphate
PO_4^{3-}	Phosphate
Pt/TiO_2	Platinum-doped titanium dioxide
2,4 DP	2,4-Dichlorophenoxyacetic acid
Pd–WO_3	Palladium tungsten oxide
$BiOBr/Fe_3O_4$	Bismuth oxybromide-doped ferric oxide
$Ag@TiO_2$	Silver titanium dioxide
SnO_2	Tin dioxide
Sb–SnO_2	Antimony-doped tin dioxide
Ag_3PO_4-$BiOCl_{1-x}Br_x$	Trisilver phosphate-doped bismuth oxychloride bromide
CM-n-TiO_2	Carbon-modified titanium dioxide
Ag/TiO_2	Silver/Titanium oxide
Ni–CuO	Nickel-doped copper oxide
$Cu{\cdot}Cr_2O_4$	Copper chromite
NiCuO	Nickel-doped copper oxide
NiCrO	Nickel-doped chromium oxide
CuCrO	Copper-doped chromium oxide
IO K-CN	Hypoiodite potassium-doped carbon nitride
IO CN	Hypoiodite-doped carbon nitride
N,S-CQD	N,S-doped carbon quantum dot
ZnO/N,S-CQDs	Zinc oxide N,S-doped carbon quantum dot
$ZnSnO_3$	Zinc stannate
NaOH	Sodium hydroxide
$ZnSn(OH)_6$	Tin zinc hydroxide
$Ag_2O/Bi_{12}GeO_{20}$	Silver oxide-doped bismuth germanium oxide
$AgNO_3$	Silver nitrate
FeOOH	Ferric hydroxide oxide
CoPc–COOH	Cobalt phthalocyanine tetracarboxylic acid
g-C_3N_4	Graphitic carbon nitride
$CdIn_2S_4$	Cadmium indium sulphide
$CdInS_4$/mpg-C_3N_4	Cadmium indium sulphide-doped mesoporous graphitic carbon nitride
RGO	Reduced graphene oxide
NiO–TiO_2	Nickel oxide-doped titanium dioxide
PyCOOH	Pyrene-1-carboxylic acid
CaO/TiO_2	Calcium oxide-titanium dioxide
ZnO/SiO_2	Zinc oxide-doped silicon dioxide
Cr/SiO_2	Chromium-doped silicon dioxide
$TiCl_2$	Titanium chloride
GCMS	Gas chromatography mass spectrometry
CZTS	Copper zinc tin sulphide
CNT–Pt/TiO_2	Carbon nanotube platinum-doped titanium dioxide
$ZnFe_2O_4$	Zinc ferrite
JNHP	Janus nanofibre heterojunction photocatalyst
ZnAl-LDH	Zinc aluminium-layered double hydroxide
$Ni_3B/Ni(OH)_2$	Nickel boride nickel hydroxide
$Y_3Al_5O_{12}@Nb_2O_5/In_2O_3$	Yttrium aluminium oxide-doped niobium pentoxide indium(III) oxide
Au/TiO_2	Gold-doped titanium dioxide
Cl-Ta_2O_5-x	Chlorine doping tantalum oxide
$MoO_3@MoS_2/TiO_2$	Molybdenum trioxide-coated molybdenum disulphide-doped titanium dioxide

Introduction

Water contamination considered being pertaining environmental issues gained pivotal attentiveness in recent years. Heavy metals, dyes and persistent organic pollutants are the three predominant pollutants occurring in nature. The presence of these pollutants in the environment even in minute amounts can pose ample health ailments in human resources. Waste discharges such as pesticide, pharmaceutical, textile and petrochemical industries routinely discharge these pollutants into the environment. Chronic toxicity, developmental and neurological disorders and cardiovascular and intestinal ailments are some of the health effects caused due to the chronic occurrence of these chemicals into the environment. Different conventional treatments exist to remediate the environmental pollutants. Some of these methods include membrane separation, solvent extraction, adsorption, filtration, electro kinetic remediation, flocculation, coagulation and precipitation (Kiruba et al. 2014; Anitha et al. 2015; Neeraj et al. 2016; Ahmad et al. 2020a; Hitam and Jalil 2020; Jeevanantham et al. 2019; Saravanan et al. 2020).

Few advanced oxidation processes include fenton reaction, photocatalysis, wet oxidation and sonolysis. Of these, photocatalysis is regarded as the suitable method due to its property of mineralising recalcitrant compounds. Photocatalysis has attracted extraordinary consideration because of its direct transformation of solar energy to the easy storage of hydrogen and CO_2 conversion to hydrocarbon fuels (Li et al. 2018). The degradation mechanism of photocatalysis has been characterised by four ways (1) light ingestion to create electron–hole sets, (2) division of energised charges, (3) transferral of electrons to the external of photocatalysts and (4) usage of charges on a superficial level for redox responses. Photocatalysis has several advantages compared to other conventional methodologies such as efficient degradation of contaminants, wastewater treatment, environmental protection, clear surface of various material, air purification and no secondary pollution. Photocatalysis study comprises the generation of chemical energy from light energy which generates charge carriers provoking redox reactions which reduce the recalcitrant pollutants. The entire process involves three major steps, namely the generation of charges, separation of charged components and their consumption (Long et al. 2020; Anandan et al. 2020; Younis et al. 2020). Pollutant degradation using photocatalyst involves four major steps: mass transfer of pollutant molecules, excitation of pollutant molecules on the photocatalytic surface, degradation of pollutant molecules by oxidised compounds and desorption of decomposed compounds from photocatalytic surface to the bulk solution. Cost efficiency, non-toxic nature, absence of further pollution and high process efficiency are the advantages of employing photocatalytic process in environmental pollutants. Electron–hole pair separation efficiency and absorption signify the dependence of good photocatalytic materials. Some of the persistent organic pollutants such as pesticides, phenol, antibiotics and herbicides are also been remediated employing photocatalytic processes. For example, glyphosate herbicide and parathion pesticide have been removed using bismuth iron oxide-based photocatalyst and titanium-based photocatalyst, respectively. In general, photocatalytic materials are confined to specific substrates. After remediation process, they consequently assist in the dispersion and recuperation from environmental platforms. Well-designed photocatalytic substrates can enhance the photocatalytic efficiency of environment pollutant remediation (Di Paola et al. 2012; Meng et al. 2015; Ayodhya and Veerabhadram 2018; Zhao et al. 2019; Wood et al. 2019; Singh et al. 2013).

Fossil fuel consumption generates the large quantity of pollutant gases which may cause toxic effect (Cheng et al. 2017; Ren et al. 2018). One of the effective explications in sustainable energy resources is the development of hydrogen fuel from solar energy by conversion and splitting of water molecules. In contrast to traditional technologies, superior efficiency and performance in energy production were observed with photocatalytic technology (Huang et al. 2019; Zhang et al. 2019a; Li et al. 2019). Biodiesel, hydrogen and methanol are some of the fuels that are being produced by using different advanced oxidation processes. Studies such as biogas, hydrogen and ethanol production using pre-treated substrates using advanced oxidation processes show the increasing interest in the emerging of advanced oxidation processes for energy production (Tamilarasan et al. 2019; Kumar et al. 2019a; Yang and Wang 2019). Several photocatalytic materials have also been utilised for the production of bioenergy and biofuels such as biodiesel, methanol and hydrogen. Few photocatalysts used for the photocatalytic water splitting include titanium oxide, bismuth oxide and ferrous oxide (Lee et al. 2019; Helal et al. 2017; Hakobyan et al. 2019).

This review describes photocatalytic materials and processes for the elimination of environmental pollutants, for example metals, dyes and persistent organic pollutants. The findings of this review would appeal to various researchers and analysts who engross on the remediation of water pollutants employing new photocatalytic materials, generation of energy by photocatalytic processes and develop their explorations towards further explicating the advancements in photocatalytic processes. The mechanism of photocatalysis and in removal of pollutants is thoroughly interpreted. Several photocatalysts developed for the elimination of toxic contaminants have been described. Additionally, the photocatalytic processes for the generation of biofuels are portrayed in detail. Current

limitations and future perspectives on the photocatalytic elimination of toxic contaminants and biofuel production are systematically discussed in this review article.

Principle of photocatalysis

Environmental pollutants can be eliminated by the process of light induced redox reactions known as photocatalysis. The exposure of photocatalyst surface to photon energy (hυ) more than or equal to band gap energy (E_{bg}) results in the agitation of electrons from valence band to the conduction band consequently leading to electron–hole pair formation in both the bands, respectively. Positive hole generated in the valence band oxidises the pollutant or water molecules producing hydroxyl radical and the adsorbed oxygen on the photocatalyst is reduced by those excited electrons. In the conduction band, excited electrons possess strong reduction ability reacting with dissolved molecular oxygen in water or adsorbed oxygen on the surface of the photocatalytic material.

Organic pollutant degradation

In case of organic contaminant, hydroxyl free radical reacts on the organic group of the pollutant and converts the toxic pollutant into non-hazardous forms (Hasanpour and Hatami 2020; Ganguly et al. 2019):

Exciting agent and reducing agent are $h\upsilon$ and h^+_{VB}, e^-_{CB} is the photon energy required to excite the electrons.

$$\text{Photocatalyst} + h\upsilon \rightarrow h^+_{VB} + e^-_{CB} \quad (1)$$

Hydroxyl radical formation

$$h^+ + H_2O \rightarrow OH^{\cdot} + H^+ \quad (2)$$

$$h^+ + OH^- \rightarrow OH^{\cdot} \quad (3)$$

Formation of super oxide radical anions and hydroperoxide radicals by reaction with oxygen

$$O_2 + e^- \rightarrow O_2^{-\cdot} \quad (4)$$

$$O_2^{-\cdot} + H^+ \rightarrow HO_2^{\cdot} \quad (5)$$

$$HO_2^{\cdot} + O_2^{\cdot} \rightarrow HO_2^- + O_2 \quad (6)$$

$$2HO_2^{\cdot} \rightarrow H_2O_2 + O_2 \quad (7)$$

$$H_2O_2 + h\upsilon \rightarrow 2OH^{\cdot} \quad (8)$$

Degradation of organic pollutants by hydroxyl radical

$$OH^{\cdot} + OP \rightarrow \text{Degraded products} \quad (9)$$

The further process of degradation is initiated by hydroxyl radicals, hydrogen ions and superoxide anion radicals (Belver et al. 2019).

Heavy metal remediation

Usually heavy metals are the prevailing pollutants in water resources. Direct or indirect reduction takes place in photocatalytic removal of heavy metals.

Direct reduction of heavy metal species by photon energy.

$$M^{n+} + e^-_{CB} \rightarrow M^{(n-1)+} \quad (10)$$

In some cases, few metal species cannot be reduced directly or be transformed to higher oxidation state. Indirect reduction by donor intermediated reduction of heavy metals

$$OH^{\cdot} + RCH_2OH \rightarrow RCHOH^{\cdot} + H_2O \quad (11)$$

$$RCHOH^{\cdot} + M^{n+} \rightarrow M^{(n-1)+} \quad (12)$$

By these reactions, heavy metals, dyes and organic pollutants can be removed in effective ways providing an alternative for conventional treatments. Metal ions or chemical species can be transformed from aqueous or contaminated solutions to photocatalytic surface removing their toxicity. Different metal ions are removed by slightly different photocatalytic mechanisms. Environmental applications of photocatalysis process are depicted in Fig. 1.

Photocatalytic remediation of environmental pollutants

Heavy metals

Globally, environmental pollution problems have been increasing every year since the industrial effluents such as organic pollutants, dyes, heavy metals and radioactive ions were discarded in the rivers, lakes and portable water. The toxicity of these pollutants causes illness to aquatic organisms and human health. These toxins are non-biodegradable. Among all these toxins, heavy metals are highly toxic and carcinogenic. They would accumulate in the food chain and affect our health. To remove these chemicals, many biological and chemical methods are used. However, photocatalytic removal processes were in practice and efficient (Sun et al. 2019; Dhandole et al. 2019). Ferric oxides are majorly used in many fields because of their stability and low cost. Three-dimensional ferric oxide hierarchical structure (3D Fe_2O_3) was synthesised for the removal of heavy metal. The 3D structure was prepared using ultrasound irradiation (Lee

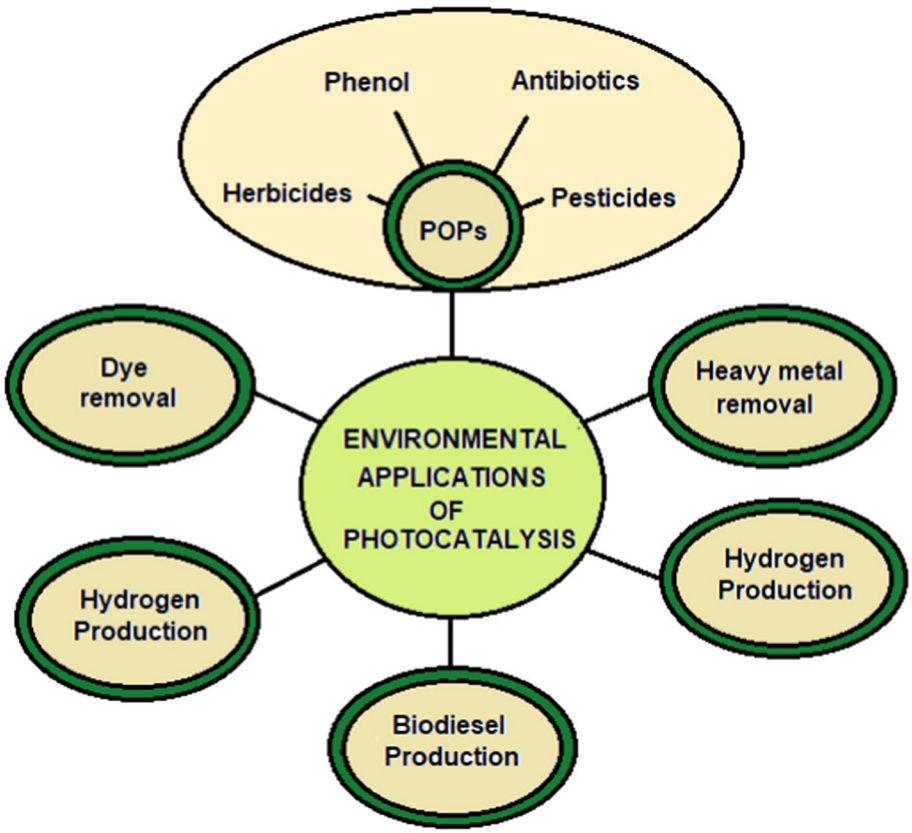

Fig. 1 Environmental application of photocatalysis process. Photocatalysis can be used for effective reclamation of contaminants such as heavy metals, dyes and persistent organic pollutants. Photocatalysis is promising technology for the direct transformation of solar energy to the easy storage of hydrogen and CO_2 conversion to hydrocarbon fuels

et al. 2018). The advantage of 3D Fe_2O_3 is that it has larger surface area, high stability and cost effective. As(V) and Cr(VI) are predominantly found in the water bodies. Source of the heavy metals for As(V) is $Na_2HAsO_4.7H_2O$ and for chromium is $K_2Cr_2O_7$. 4 mg of 3D Fe_2O_3 and 25 mL of As(V) and Cr(VI) were taken and mixed well and kept in the room temperature for 15 h. Then the removal capacity of 3D structure was analysed by plasma atomic emission spectroscopy (PAEC). The removal rate for As(V) was 100% in 6 mg of commercial Fe_2O_3, whereas in 3D-Fe_2O_3 was 100% in 2 mg. TiO_2 and ZnO were used as the source for preparing the nanoparticles for the removal of toxic contaminants. In this experiment (Shahzad et al. 2019a) $CuCo_2S_4$-modified $MoSe_2/BiVo_4$ composite was used as the photocatalyst. Hydrothermal process was used to prepare the monoclinic bismuth vanadate nanoparticles. $Bi(NO_3)_3.H_2O$ and NH_4VO_3 in 40 mL of deionised water and stirred continuously for 30 min followed by autoclave for 24 h at 180 °C. The nanoparticles were calcined at 400 °C for 3 h. From this, $CuCO_2S_4$-modified $MoSe_2/BiVO_4$ composite was prepared. To check the photocatalytic activity of the composite, chromium, copper, zinc, lead and cadmium were taken (0.1 mg of heavy metal in 100 mL of distilled water). The prepared composite also added to the container and stirred for 30 min and kept in the sunlight. The sample was drawn from the container, and removal of toxic was observed under ultraviolet visible adsorption spectrophotometry. The $CuCo_2S_4$-modified $MoSe_2/BiVO_4$ composite has photocatalytic activity under solar light irradiation.

Chemical and pharmaceutical industries discharge a large amount of heavy metals as effluent in rivers, lakes and also release CO_2 in air which causes air pollution. In this (Chen et al. 2020) work, a new unfamiliar idea was introduced. The heavy metals are removed using adsorbents, and then the removed heavy metals are used as the photocatalyst for the reduction of CO_2. Removal of heavy metal was attained by calcium silicate hydrate nanosheets. It was prepared using the rate controlled precipitation method. Four major heavy metals were selected (Cu^{2+}, Zn^{2+}, Ni^{2+}, Pb^{2+}). Calcium silicate hydrate nanosheets have high stability and high adsorbent capacity. The heavy metal solutions ($Cu(NO_3).3H_2O$, $Zn(NO_3)_2.6H_2O$, $Ni(NO_3)_2.6H_2O$, $Pb(NO_3)_2$) are added to 20 mg of calcium silicate hydrate ultrathin nanosheets and the experiment carried out at 25 °C and pH 5.0. The solution was stirred continuously. After 30 min, 1 mL of solution was centrifuged and to the supernatant 2% of HNO_3 was added and the adsorption was viewed in atomic adsorption spectrometry. The removal of heavy metal in calcium silicate hydrate nanosheets was efficient, and sheets were washed with distilled water, ethanol and used as photocatalyst for the CO_2 reduction. In another studies, rhodium and antimony codoped TiO_2 nanorod (Rh–Sb TiO_2) and titanate nanotube

composite (RS-TONR/TNT) degrade organic pollutant and remove heavy metals in water under sunlight irradiation. Molten salt flux method was efficient for the synthesis of Rh–Sb codoped TiO_2. For composite (RS-TONR/TNT) preparation, hydrothermal is considered to be convenient technique. Lead, copper, zinc and cadmium metal ions were chosen and added separately to the 25 mg/L of prepared composite. The solution was allowed for the adsorption process under the sunlight, and the ion concentration was observed in plasma atomic emission spectrometry. Lead ion has adsorbed in higher rate, and zinc ion was least adsorbed metals. Preparation methodology of TiO_2 photocatalyst is listed in Table 1.

Cr(VI) is highly toxic and very difficult to remove from the water bodies (Zhang et al. 2019b). Nano-heterojunction ($AgIn_5S_8/Bi_2WO_6$) was prepared by adding $Bi(NO_3)_3$ and Na_2WO_4 solutions in $AgIn_5S_8$ of different mass percentage such as 5%, 10%, 15%. To study this removal experiment, pure Bi_2WO_6 and pure $AgIn_5S_8$ and $AgIn_5S_8/Bi_2WO_6$ were compared. The concentration of chromium was analysed by means of diphenyl carbazide method. Pure Bi_2WO_6 removes 54%, and $AgIn_5S_8$ removes 68% and 10% of $AgIn_5S_8/Bi_2WO_6$. Pure Bi_2WO_6 results in 22% reduction, 5%, 10% and 15% of $AgIn_5S_8/Bi_2WO_6$ terminate 43%, 54%, 64%, respectively, and pure $AGIn_5S_8$ shows 98% of chromium reduction.

Pyrite (FeS_2) is natural iron sulphur mineral. In mineral separation process, the pyrite was discarded as tailing waste. It has higher capacity in the removal of environmental pollutants. Usually, FeS_2 was used as semiconductor adsorbent. FeS_2 was used as the photocatalyst for concurrent removal of heavy metals and dyes and degradation of the organic pollutant (Diao et al. 2015). For the photocatalytic reactions, 1 g/L of FeS_2 was suspended into the solution containing malachite green and Cr(VI). Ultraviolet lamp was used for the photocatalytic irradiation, and the whole experiment was carried out in a reactor. Prior to the photocatalytic activity, the solution was subjected to the stirring process for 30 min using a magnetic stirrer. The initial concentration of malachite green dye and Cr(VI) ion was noted. The photocatalytic activity was carried out for 120 min. Organic pollutants were degraded separately using different photocatalyst. In this experiment (Yuqing et al. 2020), Z-scheme BiOCl–Ag–AgBr photocatalyst was synthesised to degrade organic pollutant. BiOCl nanosheets were synthesised by the modified solvothermal method. Then BiOCl–Ag was prepared using photodeposition method by loading Ag on BiOCl. Under solar irradiation, the experiment was carried out. 50 mg of photocatalyst was dispersed into 50 mL of Cr(VI) ion and phenol solution. After that, the experiment was carried out and samples were withdrawn and analysed using diphenyl carbazide colorimetric method. BiOCl–Ag–AgBr has high removal efficiency compared with others.

Dyes

Dyes are most common effluent that is discharged from the pharmaceutical, chemical and textiles industries. These effluents contain many toxic and carcinogenic compounds that cause illness to humans and ecosystems. Photocatalytic removal process is the excellent way to reduce the toxicity in the wastewater containing heavy metals and dyes and convert them into nontoxic compounds (Eckert et al. 2015). Many textile, chemicals and food industries release toxic dyes into the portable water and rivers. In this experiment (Soliman et al. 2017), transition metals and activated carbon were combined together and used for the removal of the crystal violet that was released from the industries. Activated carbon was prepared from the agriculture waste. Further the transition metals were doped on the surface of the activated carbon by ion exchange process. Different metal ions are used, namely cadmium, zinc, copper and lead. 5 g of activated carbon was added to each container containing 500 mL of metal solutions and kept in the shaker for 20 h. From each container, 1 g of sample was taken and 250 mL of crystal violet dye was added and kept in the dark for 20 h in the shaker and kept in solar light. The concentration of activated carbon was noted. The photocatalytic activity of these metal ions with activated carbon shows better results.

Sodium iron disulphide ($NaFeS_2$) was a good semiconductor and utilised as a catalyst in wastewater treatment. In this (Dileepkumar et al. 2020) work, the photocatalytic material was prepared by hydrothermal process. During the synthesis of $NaFeS_2$ and $NaNO_3$, by-products are removed and the yield was around 55%.

Table 1 Methods for TiO_2 photocatalyst preparation

S. no	TiO_2 preparation methods	Advantages	Disadvantages	References
1	Hydro thermal method	1. Cost effective 2. Low energy consumption	1. Need expensive autoclave 2. Reusability is a tedious process	Wong et al. (2011)
2	Sol Gel method	1. Easy preparation 2. High surface area	1. High precursor cost 2. Product bondage is weak	Sood et al. (2015)
3	Coating method	1. Efficient 2. Rapid method	1. Difference in thickness of coated layer	Nickheslat et al. (2013)

$$Fe(NO)_3 \cdot 9H_2O + Na_2S \cdot 9H_2O + NaOH \rightarrow NaFeS_2 + NaNO_3 + H_2S \quad (13)$$

Various experiments were carried out to check the photocatalytic effect of $NaFeS_2$ on methylene blue dye. The $NaFeS_2$ catalyst was added to the methylene blue dye solution and kept under ultraviolet radiation. The results show negligible decomposition of dye. 250 mL of methylene blue dye and indigo carmine dye were separately taken in the circular photoreactor and 60 mg of photocatalyst was added and kept in the ultraviolet radiation and the samples were drawn at a certain interval and the decomposition was observed. At 105 min, the methylene blue shows the maximum decomposition of dye 97% and indigo carmine shows 99% decolourisation of dye at 45 min. This experiment shows that when the time increases, the decolourisation also increases. Hence, $NaFeS_2$ was considered to be a good photocatalytic material.

TiO_2 was the most commonly used photocatalyst for the degradation of organic pollutants (Gusain et al. 2019). As per (Sood et al. 2015) work, titanium oxide quantum dots (TiO_2 QD) were prepared by solgel process. The photocatalytic activity was done in the ultraviolet chamber using the batch reactor. To maintain the temperature of 25–30 °C, water circulation was given externally. The quantum dots and 25 mg/L of indigo carmine were taken to test the removal capacity. In the presence of catalyst, the removal study was found to be 93% in 120 min. This experiment concludes that TiO_2 quantum dots were used as the photocatalytic material. Metal and metal oxides are used for the removal of the dye and organic pollutant. Copper oxide nanoparticles (Cu_2O NPs) are used to remove the methylene blue dye from the aqueous solution. The raw materials used for the synthesis of Cu_2O nanoparticles are Cu^{2+} and *Terminalia arjuna* bark extract. 100 g of bark was taken and washed with 100 mL of double-distilled water; the bark pieces were added, and the condenser was connected. The whole set-up was placed in the microwave irradiation for 7 min. From the stock solution, 10 mL was taken and 50 mL of $Cu(NO_3)$ was added and kept in the microwave irradiation. After certain period, the reaction between them takes place and Cu_2O NPs were synthesised. 20 mg of Cu_2O in 200 mL of methylene blue dye solution was stirred continuously. Readings were noted over certain period of time under ultraviolet–visible spectrophotometry (Kangralkar et al. 2019).

As per (Zhang et al. 2015) work, TiO_2/MoS_2 was fabricated on zeolite using the ultrasonic hydrothermal process. Titanium tetrachloride ($TiCl_4$) was used as titanium source, molybdenum sulphide (MoS_2) as sensitiser. The photocatalytic activity of TiO_2/MoS_2@zeolite was tested using methyl orange as the toxic pollutant. The removal capacity was compared with Degussa P25. It was used as the referred photocatalyst to evaluate the photocatalytic activity. TiO_2 is an efficient photocatalytic material for the removal process, and MoS_2 acts as a semiconductor because of its stability towards photocorrosion. 4 mL of $TiCl_4$ and MoS_2 powder were added into the beaker using ultrasound process, and homogenised solution was obtained. Glycerol was added, and the solution was subjected to continuous mixing; finally, zeolite was added. The whole solution was transferred into the autoclave, and hydrothermal process was done. After the process, the photocatalyst was obtained. To check the activity of the photocatalyst, 20 mg/L of methyl orange and 125 mg of photocatalyst were added into 250 mL of organic solution. The solution was stirred continuously for 30 min prior to the reaction to attain the equilibrium. The experiment was carried out in a reactor under XG500 xenon long arc lamp at acidic pH. At every 10-min interval, the samples were withdrawn from the reactor and analysed by spectrophotometer at absorbance of 464 nm. The concentration of photocatalyst varies from 0.25 to 0.80 g/L. The removal is high in acidic pH as pH goes into basic the activity decreases. The results of photocatalyst were compared with pure zeolite, Degussa P25, TiO_2@zeolite, and the removal was 1.5%, 55%, 77%, respectively. This result shows that TiO_2/MoS_2@zeolite has excellent activity over removal of the methyl orange dye. The Sm@POA–TP is an efficient and reusable catalyst (Manea et al. 2019). The removal of methylene blue and malachite green dye was studied using the Sm@POA–TP catalyst. The prepared POA was added to the solution mixed constantly and kept in the room temperature for 24 h. POA–TP mixture was filtered, washed with distilled water and dried in an oven to obtain the product. 0.01 M Sm(III) was doped on POA–TP at room temperature and stirred constantly for 2 h using a magnetic stirrer. Then the solution was washed with distilled water and dried to obtain the final product. Sm@POA–TP and 200 mg/100 mL of methylene blue, malachite green dyes were added into the reactor container, and 500 W light source was given. Then the reaction proceeds, and aliquots of samples were collected and analysed in ultraviolet–visible spectrophotoscopy. The removal was about 94% and 90% for methylene blue and malachite green dyes, respectively, after 4 h of light irradiation.

Persistent organic pollutants

Organic pollutants are originating from petrochemical plants, urban sewages, pharmaceutical industries and agro-industries activities. Petrochemical plants mainly release atomic hydrocarbon, detergents, antibiotics, phenols and its derivatives. These organic pollutants are released in

aquaculture water, drinking water, rivers, soils and seas (Shahidi et al. 2015). Organic pollutants should be treated, and hazardous chemicals are removed before discharging the wastes from the industries.

Pesticides

Pesticide is one of the most common and hazardous organic pollutants used in agricultural lands. Pesticides are made up of organic and non-organic (chemicals) compounds which are used to destroy the pests in the land and protect the crops so that the farmers get higher yield. But due to the excessive use of the chemical pesticides, the toxic compound remains active in the farms and also in the crops which causes dreadful illness to the mankind. Many methods are in practices to degrade the toxicity of pesticides in the land such as nano-based catalyst, nanofiltration and nanocomposites (Khan and Pathak 2020).

Carbamate pesticides are widely used in agriculture fields to control pests. TiO_2 is used as the photocatalyst which helps in the degradation of pesticides from the lands. From the work of Kanan et al. (2019), TiO_2 has a unique structure in which the titanium ions have an active site that degrades the organic pollutants. At a specific optimum condition, the TiO_2 gives the maximum degradation of pesticides. TiO_2 shows 20% increased degradation activity along with the ultraviolet irradiation activity. Also when catalyst (H_2O_2) was added to the TiO_2/UV, the degradation of carbamyl was recorded as 79% without catalyst the degradation was 41%. This shows that the TiO_2 has maximum degradation at specific conditions such as catalyst, temperature, pH and ultraviolet irradiation. Monocrotophos and chlorpyrifos are widely used organo phosphorus pesticide. As per (Amalraj and Pius 2015) work, TiO_2 nano-photocatalyst was synthesised using the solgel process. The photocatalyst and pesticides were mixed and placed in a glass jacket and immersed in the batch reactor. The variation of monocrotophos and chlorpyrifos concentration was determined using the ultraviolet–visible spectrophotometer. O_2 and H_2O are reacting on the TiO_2 surface and thus forms an HO* radical, which has the ability to degrade the monocrotophos and chlorpyrifos. As per (Ayodhya and Veerabhadram 2019) work, ZnS nanoparticles are synthesised using a Schiff base which acts as a capping agent. Under ultraviolet irradiation, the chlorpyrifos degradation was evaluated using the Schiff base ZnS nanoparticles. The photocatalyst and the pollutant chlorpyrifos were mixed and the reaction carried out in the photoreactor. The mixture should attain the adsorption equilibrium, for that continuous mixing was done for 10 min. Then the set-up was kept in the ultraviolet light irradiation. The degradation of the chlorpyrifos was analysed, and the comparative study was done between the normal ZnS and Schiff base ZnS nanoparticles. Under ZnS, the degraded recorded as 56.34% in 60 min, whereas in Schiff base ZnS nanoparticles the degradation was 85.29%. The above results show that Schiff base capped ZnS NPs are used as a photocatalytic degradation material. Degradation of dicofol was experimented by using nanocomposite. The photocatalyst and the organic pollutant were combined and treated under ultraviolet light. Without photocatalyst, the degradation of pollutant was less. The nanocomposite catalytic activity remains active after 5 cycle of usage (Ahamad et al. 2019).

O,O-dimethyl-S-methyl carbamoyl methyl thiophosphate commonly known as omethoate is a type of pesticides majorly used in developing countries. Due to its high toxic content, biological and traditional methods are not used to degrade this compound. According to Mohamed et al. (2020) work, nanocomposite was prepared using silica fume-based MCM-41, cobalt oxide and pomegranate leaves extract. Pomegranate leaves extract acts as a reducing agent. 0.51 g of CTAB and 16.34 mL of NH_3OH were dissolved in 25 mL of distilled water and stirred over a period of time. Further 0.75 g of silica fumes was added to the solution and mixed well for 30 min at 1000 rpm. After that, the solution was kept in the autoclave and heated at 100 °C for 24 h. After the filtration process, the MCM-41 was prepared. The pomegranate leaves were powdered, and 5 g of powder was added to the distilled water and boiled for 3 min and filtered to obtain the pomegranate leaves extract. 2 g of MCM-41 was added to the 50 mL of distilled water and stirred for 30 min, then 2.5 g of $Co(NO_3)_2{\cdot}H_2O$ was added slowly, and 50 mL of pomegranate leaves extract was also added. The solution was stirred continuously for 12 h and filtered to obtain the nanocomposite. The experiment was carried out in a glass chamber with a metal halide lamp for light source. The green nanocomposite and omethoate were added into the reactor and kept in dark for 30 min to attain the equilibrium. After the reaction process, samples were collected and analysed by high-pressure liquid chromatography (HPLC). At different catalyst dosage such as 0.1, 0.15, 0.2 and 0.25 g at constant 100 mg/L of omethoate, complete degradation occurs at 100, 70, 60 and 50 min. Likewise, for different concentrations of omethoate from 50, 100, 150, 20, 250 mg/L at 0.25 nanocomposite complete degradation occurs at time of 30, 50, 80, 100 and 120 min. From the results, it clearly shows Co_3O_4/SF–MCM-41 has excellent photocatalytic activity. Parathion pesticide was widely used in the agricultural lands. TNP-Pd-Fe_3O_4/GO and used for the degradation study for the parathion pesticide present in the waste water (Saljooqi et al. 2020). Pd (Palladium) nanoparticles were used to stabilise TiO_2 nanoplates. 100 mg of TNP-Pd nanosheet was dissolved in 20 mL ethanol, and 50 mg of Fe_3O_4 was dispersed in 50 mL of ethanol. Then one mixture was added into the other slowly and stirred for 6 h at 40 °C. The experiment was performed under ultraviolet light, and samples were collected and analysed under ultraviolet–visible spectroscopy at

absorbance of 260 nm. The photoactivity of the difference nanoparticles was investigated, and titanium nanoplate and TNP-Pd degrade within 80 min and 60 min, respectively, whereas the TNP–Pd–Fe_3O_4 nanosheets degrade the pesticide in higher speed and takes lower time. The degradation efficiency was recorded as 98.5%, and the products obtained were CO_2, SO_4^{2-}, PO_4^{3-}, H_2O which were harmless for the environment.

Herbicides

Pesticides and herbicides are mainly used in the agricultural land to control the pest attack which affects the yield of the crops. Higher usage of these chemicals over a prolonged period of time affects the soil fertility and the water resources. Among all herbicide 2, 4-dichlorophenoxyacetic is more toxic and carcinogenic. The degradation of this compound is difficult to remove because of its stability and less water solubility nature. The best method for the removal of herbicide pollutants is the photocatalytic degradation process (Sobahi 2017). Using Pt/TiO_2 nanoparticles, the 2,4-D (2,4-dichlorophenoxyacetic acid) and 2,4-DP ((2,4-dichlorophenoxy)propionic acid) herbicides were degraded. Using the solgel method, TiO_2 and Pt were synthesised. Cylindrical quartz glass of 10:20 height and diameter of photoreactor was used for the degradation process. After the process, the degradation was analysed using ultraviolet–visible spectroscopy. The degradation of pollutants is high in platinum-loaded titanium oxide than the free titanium oxide (Abdennouri et al. 2015).

High dose usage of herbicides leads to the contamination of the water bodies and soils. It can be effectively degraded using photocatalytic activity. As per (Zahedi et al. 2015) work, N,S codoped TiO_2 thin films were used for the degradation of paraquat herbicide. Initially, TiO_2 is prepared using the solgel process, and from TiO_2 the thin films of TiO_2 were prepared by using glass beads as the base. The surface of the glass beads should be free from organic and non-organic material, for that the beads were washed in deionised water and dried. The glass beads are then soaked in the TiO_2 solution for 10 min and air-dried to obtain the immobilised TiO_2. The degradation was performed in the photoreactor. The beads were arranged in the bottom of the reactor, and through an external valve the pollutant was added and samples were drawn from the reactor and analysed. The results show that under the sunlight degradation was 54.84%; on other hand, under ultraviolet the degradation of herbicides was observed as 74.1%.

Herbicides are categorised under pesticide pollutants. It also contaminates the water bodies. Diquat is a type of herbicide marketed as dibromide salt. In this experiment (Shibin et al. 2015), The ZnO acts as the photocatalyst and the reactor vessel consists of 50 mg/L of diquat solution, 0.6 mg/L of ZnO and external water supply was given to maintain the temperature. The set-up was kept in the solar light. During this process, OH* radicals are formed on the surface of the ZnO and it is tested by photoluminescence. The photocatalytic activity of ZnO degrades 58% of diquat pollutant in 5 h. Hence, ZnO is used as the photocatalytic agent. S-triazine is degraded using TiO_2 suspension as a photocatalyst. Herbicide is used as an additive in paints to reduce the algae growth. This experiment was carried out in a stirred tank reactor. 10 mg/L of S-triazine herbicide and 100 mg/L of TiO_2 into the reactor and agitated continuously and then kept in dark for 30 min before placing it in the sunlight. At every 10-min interval, samples were taken and TiO_2 particles were removed using nanofiltration and samples were dried. The sample was analysed using gas chromatography. The results show that TiO_2 perform the degradation activity effectively under sunlight (Konstantinou et al. 2001).

To increase the crop yield and inhibit the insect pest, herbicides are predominantly used (Mkhalid 2016). Using hydrothermal process, tungsten trioxide was synthesised and palladium (Pd) metal was decorated on the surface by photo-assisted process. The photocatalytic activity of the catalyst was checked by degrading (2,4-D) 2,4-dichlorophenoxyacetic acid under ultraviolet irradiation. Degradation capacity of both tungsten trioxide and Pd–WO_3 was separately dispersed in 200 mL of 2,-D solution and subjected to uniform stirring before the photocatalytic activity. After certain time intervals, samples were taken and analysed using HPLC. The degradation percentage of Pd after 90 min along with tungsten trioxide for 0.0, 0.05, 0.10, 0.15 wt% was 73%, 79%, 85% and 100%. Reusability efficiency was checked and shows constant degradation activity for 5 cycles. Glyphosate (*N*-(phosphonomethyl) glycine) was an active organo phosphorus compound; due to its strong soil binding capacity and high resistant to the molecules, degradation by biological process was difficult. As per Cao et al. (2019) work, phosphonomethyl glycine was degraded using magnetic BiOBr/Fe_3O_4 nanocomposite as the catalyst. The catalyst was synthesised using the solvothermal method. A 500-W xenon lamp was fitted in the centre of the circulating plate and water circulated around the vessel. 0.08 g of catalyst was added to 20 mL of phosphonomethyl glycine. 8 tubes are fitted around the lamp. Air flow in the form of bubbles was sent into the tubes, and continuous stirring is done during the reaction and also before the reaction for homogenous mixture. After the photocatalytic activity, the magnetic catalyst was separated using a magnet. The samples were withdrawn and analysed under ion chromatography. The results show that 9% degradation for BiOBr/Fe_3O_4 and it was compared with pure BiOBr and Fe_3O_4 and the results were 85% and 5%, respectively. From the study, it was concluded that magnetic BiOBr/Fe_3O_4 has higher degradation capacity and it can be used as the photocatalyst. Up to 5 repeated cycles

of degradation process, the photocatalyst has an average of 90% degradation; this shows it has reusable property.

Phenols

Phenol and phenolic compounds are considered to be major organic pollutant in the water bodies and cause ill effects in the aquatic system. Phenol is the most abundant organic pollutant in wastewater. Many methods are used for the removal of toxic phenol from the water environment. Photocatalytic degradation is one of the successful methods. Semiconductor is usually used as a photocatalyst (Dewidar et al. 2018).

The phenolic compounds are mainly released from petroleum and pharmaceutical industries, and they remain toxic for a longer period. In this (Shet and Vidya 2016) study, the phenol was degraded by the fluidised bed reactor using immobilised nanoparticles. Phenol was stored in the tank and pumped into the reactor through the peristatic pump. The reactor was packed with glass beads up to 5 cm. Above the glass beads, a thin cellulose acetate film flakes with immobilised nanoparticles are placed. The immobilised nanoparticles were synthesised from Ag and TiO_2 using the one-pot synthesis method. Ag@TiO_2 is a core shell structured nanoparticle. 1000 mL of 10 mg/L of phenol is distilled in water, and the set-up was kept in the open terrace and was operated in between 10 AM to 5 PM to obtain the sunlight. The phenol degradation was observed. In the absence of catalyst, the phenol removal is noted as 113%. Hence it is concluded that Ag@TiO_2 can be used as the solar photocatalytic degradation of phenol.

Solar degradation is commonly used for phenol degradation, but it is very less effective because of large band gap. In Al-Hamdi et al. (2016) study work, the photocatalytic degradation of phenol was studied by HPLC. Initially, antimony (Sb)-doped tin dioxide (SnO_2) nanoparticles were synthesised using the solgel process at a low temperature and photocatalytic activity for phenol was studied under ultraviolet light and solar irradiation. Sb and SnO_2 are n type dopant and n type semiconductor, respectively. By using different concentrations of Sb doped on the SnO_2, the photocatalytic activity of nanoparticles is checked and phenol was used as the test contaminant. From the results obtained, the Sb–SnO_2 nanoparticles degrade almost 95% phenol concentration and they can also be used in the photocatalysis field. Ag_3PO_4-$BiOCl_{1-x}Br_x$ composites were synthesised using a facile two-step process. The degradation process was done using the synthesised material under sunlight irradiation. Ag_3PO_4 is coated on the $BiOCl_{1-x}Br_x$. The composite was placed under solar irradiation, and the degradation activity was carried out. A 300-W Xe lamp was the light source. In phenol solution, the photocatalyst was added and the suspension was irradiated and the results were obtained. Only Ag_3PO_4 material under the solar light showed 7.3% degradation in 75 min. At 75 min of irradiation, $BiOCl_{0.75}Br_{0.25}$ showed 72.4% degradation and the composite of ratio Ag_3PO_4-$BiOCl_{0.75}Br_{0.25}$ (1:5) degraded almost 97.9% of phenol as per (Qi et al. 2018) work. From the work, it is concluded that Ag_3PO_4-$BiOCl_{0.75}Br_{0.25}$ has the photocatalytic activity to degrade the phenol. In seawater, the degradation of phenol was obtained using carbon-modified titanium dioxide (CM-n-TiO_2) nanoparticles under ultraviolet light and solar light. In Shaban et al. (2013) work, initially the unmodified titanium oxide and carbon-modified titanium oxide nanoparticles were synthesised using the solgel method. Seawater sample was taken and initial phenol concentrations were noted. The nanoparticles were added to the sample and the photocatalytic experiment was performed over a period of time and the phenol degradation was observed. In regular unmodified n-TiO_2, the degradation of phenol was 42.26% in 240 min, whereas in modified CM-n-TiO_2 under both ultraviolet and solar light it shows effective degradation. Complete degradation occurs in ultraviolet light in 180 min. This shows that the carbon-modified titanium oxide nanoparticle has efficient degradation of phenol and degrade at an optimum pH assortment of 3.0.

Using ultrathin magnesium oxide-coated Ag/TiO_2 (Silver/Titanium oxide) nanoparticles, the degradation of phenol experiment was carried out (Scott et al. 2018). TiO_2 nanorods were synthesised by using hydrothermal process. Further, Ag/TiO_2 nanoparticles were prepared by coating Ag nanoparticles on TiO_2 nanorods and then a thin layer of magnesium oxide was coated on Ag/TiO_2 using atomic layer deposition process. To inspect the activity of photocatalyst, 10 mg of photocatalyst was added to the 50 mL solution of 15 mg/L of phenol and kept in the ultraviolet irradiation. After 30 min, the sample was collected and the catalyst was filtered. By increasing the layer of magnesium oxide on Ag/TiO_2, the light absorbance was increased that enhances the photocatalytic activity. The efficient thickness of magnesium oxide for the degradation of the phenol was determined by the followed protocol. 0, 1, 5, 10 and 20 cycles of atomic layer deposition were tested. It is confirmed that 5 cycles of magnesium oxide coated on Ag/TiO_2 were efficient. The degradation capacity has reached 95% in 120 min. After 5 cycles of atomic layer deposition, the degradation graph gradually decreases. Only Ag/TiO_2 nanoparticles act as catalyst, the degradation was 87%.

In the experiment (Rani and Shanker 2018), a natural surfactant water (*Aegele marmelos* leaf extract) was synthesised and used along with bimetallic oxide as a photocatalyst. The bimetallic oxide used in the experiment was Ni–CuO, Cu·Cr_2O_4 (copper chromate) and $NCrO_3$. Fresh *A. marmelos* leaves were collected, ground and dissolved in deionised water to obtain the plant extract. Equimolar amount of leaf extract was added to the 2nd metal salt solution (0.05 M, 100 mL) and dropwise the solution is added

to the 1st solution (0.05 M, 100 mL) under continuous stirring for 2 h at 80 °C. Further dilute ammonium solution was added to the metal oxide mixture until the precipitation occurs. The solution is filtered, washed and dried. 5–25 mg of bimetallic nanocomposite of different doses on selected phenol solution of concentration varied from 1×10^{-4} M to 1.8×10^{-4} M at different pH (3.0, 5.0, 7.0, 9.0 and 11.0). Final sample solution has 15 mg of catalyst and 50 mg/L of phenol at neutral pH under solar irradiation. After the process, the samples were collected and examined under ultraviolet–visible spectrophotometer. Lower concentration of $1x10^{-4}$M shows the effective result. At high concentration, the phenolic compound absorbs sunlight rather than photocatalyst. The effective degradation of bimetallic oxide is in the order: 3-aminophenol > phenol > 2,4-dinitrophenol. The reusability property of catalyst was investigated; the photocatalyst was removed and then subjected to acetone and the deionised water washing and dried at 60 °C for 30 min. Slightly efficiency variation in 3-nitrophenol adsorption. After the 10th cycle, 93% Ni–CuO, 91% NiCrO and 88% CuCrO degradation was recorded. High degradation was observed in NiCuO at neutral pH.

Antibiotics

Antibiotics are manufactured in pharmaceutical industries and used in the hospitals. Unused, remaining and expired antibiotics are discharged in the lands and water. It affects the ecosystem and the fertility of the soil. Macrolide antibiotics are commonly found antibiotics in the water worldwide, due to its low water solubility nature (Babic et al. 2017). Antibiotics residues are not properly treated through wastewater treatment plants. Titanium oxide is most commonly used for the degradation of organic pollutants because of its effective photocatalytic activity and low cost (Do et al. 2019; Oliva et al. 2020).

As per Lei et al. (2020) work, antibiotics are degraded using photocatalyst. Fluoroquinolone antibiotics are degraded using inverse opal potassium-doped carbon nitride (IO K-CN). Fluoroquinolone includes levoflavin and norfloxacin. SiO_2 photocatalysts is used as a template for IO K-CN preparation. K undoped (IO CN) was used as the control.

Control: 50 g antibiotic in water matrix in 20 min dark. Then it is allowed to irradiate under the xenon lamp of 300 W. After irradiation, the samples were collected and the levoflavin and norfloxacin were analysed using HPLC. Photocatalytic degradation: 50 mg photocatalyst in 50 mL antibiotic and kept in 20 min dark. Then, the procedure continues as the same as control and the samples were analysed. All IO K-CN showed better results; in particular, IO K-CN (7.5) has shown the highest degradation. In Qu et al. (2019) work, surface functionalised N,S-doped carbon quantum dot (N,S-CQD) was designed and synthesised by the hydrothermal process, where the carbon source is cysteine. The quantum dot was inserted in ZnO nanoflowers. 20 mL of organic pollutant solution was added to the photocatalytic device, and 10 mg of ZnO/N,S-CQDs sample was added to attain the adsorption equilibrium. Then, the sample was irradiated by sunlight and the sample was examined by the ultraviolet–visible spectrophotometer. Finally, the wok concluded that the organic pollutant removal was 79% after 120 min of ZnO/N,S-QCDs under ultraviolet irradiation, whereas 22.8% in ZnO and 9.3% in carbon-doped quantum dots.

Perylene diimide supramolecular photocatalyst is a 3D network structure, which has higher degradation capacity and adsorption. Firstly, the 3D network perylene diimide supra-molecular photocatalyst was prepared and the reaction for the degradation takes place in a multichannel photochemical reactor system. 25 mg of photocatalyst dissolves in 50 mL of antibiotic solution. Before exposing into the ultraviolet radiation the mixture was analysed in ultraviolet–visible spectrophotometry. The degradation capacity of 3D network perylene diimide supramolecular photocatalyst for tetracycline was found as 0.433/h. Thus, 3D network perylene diimide supramolecular photocatalyst has the degradation activity (Zhang et al. 2020). The synthesised double shelled $ZnSnO_3$ hollow cubes acts as photocatalyst (Dong et al. 2019). It was prepared by co-precipitation method. Solution A: 0.4 g stannic chloride and 5 mL of ethanol solution. Solution B: 0.15 g sodium citrate, 0.1 g zinc chloride and 10 mL distilled water. After preparation of 2 solutions both were mixed well and 20 mL of 0.4 M NaOH solution was added, stirred for 1 h. Further, 10 mL 2 M NaOH was added to the mixture to form $ZnSn(OH)_6$ double-shelled cubes. This catalyst not only degrades ciprofloxacin, but also degrades other pollutant such as toxic dyes. The experiment was carried out in reactor with 300 W xenon. 25 mg of photocatalyst and 50 mL of pollutant solution were mixed and poured into the reactor for the degradation reaction. At different intervals, samples were collected, filtered in centrifuge and analysed in ultraviolet–visible spectroscopy. The pollutant degradation was recorded as 85.9%, 37.5%, 96.52%, 48.3%, 34.8% for ciprofloxacin, sulphamonomethoxine, methylene blue, rhodamine B and methyl orange, respectively. Using hydrothermal method; $Ag_2O/Bi_{12}GeO_{20}$ heterostructure were synthesised and acts as photocatalyst for the removal of toxic contaminants (Ruan et al. 2018). The degradation results were compared with pure $Bi_{12}GeO_{20}$ material to check the efficiency of the photocatalyst. To obtain the $Bi_{12}GeO_{20}$, the suspension was centrifuged and dried. Followed by heterostructure preparation, $Bi_{12}GeO_{20}$, distilled water and 0.6 g NaOH solution were added and stirred for 1 h; further, 0.0013 mol $AgNO_3$ was added under dark condition and stirred constantly for 12 h to obtain the heterostructure product. 50 mg of photocatalyst was added with 100 mL of tetracycline, ciprofloxacin and levofloxacin

solution and sonicated for 15 min. To attain the equilibrium of the solution, it was kept in the dark for 30 min. After the reaction, samples were collected and examined under ultraviolet–visible spectroscopy. The recorded results were compared with pure $Bi_{12}GeO_{20}$ and found that for tetracycline, ciprofloxacin and levofloxacin the degradation rate was 4.5, 3.5 and 4.7 faster, thus confirming that it has efficient degradation capacity. Different photocatalysts used for pollutant degradation are listed in Table 2. Figure 2 shows that heavy metals and organic pollutants degradation by photocatalysis process.

Photocatalysts and processes for fuel generation

Methanol

Methanol is an alcohol which is also used as fuel for various purposes. It has less energy density and is less expensive but also more toxic compared with ethanol. So, when it is used as fuel, there is always a mixture of other fuels with methanol. This fuel can be synthesised with carbon dioxide, and hydrogen and bio methanol can be produced by gasification of organic substrates. It is used in cooking, racing cars and combustion engines in many countries. For a higher yield in photocatalytic reactions, the factors that can influence are higher surface area of catalyst, high light absorption, prolonged presence of catalyst and selectivity. Amorphous FeOOH coupled with m-WO_3 has been used as photocatalyst for the fuel generation was prepared by KIT-6 silica in Juan et al. (2020) and Yang et al. (2020). Many parameters of the catalyst material were analysed, like crystalline structure, morphology, catalytic performances, and textural properties; most of them showed positive results. Only methanol was observed in higher amounts, and other few compounds were present in trace amounts. The conversion rate of CH_4 was increasing with the input FeOOH. Also, it was found that the conversion of m-WO_3 with FeOOH was 3 times greater than without it. The CH_4 conversion increase was probably due to the coating of FeOOH which probably enhances photocatalysis. As there were different proportions of FeOOH used, the most preferred one, i.e. having the highest yield, was 1.98% with a selectivity of 91%. Moreover, the incident light intensity was found to be one of the factors influencing the activity of the photocatalyst. When the intensity was low, the yield was low as well, and when intensity was increased, the oxidation of methane occurred. But when the intensity is increased very high, the selectivity for methanol got reduced and carbon dioxide was increased. After this, the stability of the catalyst was analysed, and results showed that the catalyst performance was slightly reduced, while recycling run was done. In conclusion, anchoring was proven to be advantageous.

As per Kumar et al. (2019b)'s work, methanol was seen the highest product column and other by-products like formic acid were not found. Here, three catalysts have been used: CoPc–COOH, *g*-C_3N_4, and *g*-C_3N_4/CoPc–COOH which were studied, and the yield for each of them was calculated. The combined catalyst (*g*-C_3N_4/CoPc–COOH) gave the highest yield leaving behind a very far second CoPc–COOH. After this, the different proportions of *g*-C_3N_4/CoPc–COOH were tested: 5%, 10%, and 15%. The 10% was found to have higher yield due to less concentration of photosensitiser in 5% and excess concentration of 15% which led to leaching. For checking whether the yield was because of photoreduction of CO_2 or not, blank experiments were conducted: Firstly, photoreduction with and without photocatalyst, and secondly, photoreduction by photocatalyst in dark. And all the results pointed to the photoreduction of CO_2 using photocatalyst for methanol production. Then, isotope labelling, stability testing was also performed, and results were positive. Finally, the interaction between -COOH group and carbon nitrate atoms were proven to be the reason for better yield.

Another photocatalyst used by Liu et al. (2017), $CdIn_2S_4$ and $CdInS_4$/mp*g*-C_3N_4 composites produced methanol as a product. The bare $CdIn_2S_4$ produced significantly lower yield than the combined one, and the increase in mp*g*-C_3N_4 (mesoporous *g*-C_3N_4) enhanced the yield too. But, after a certain amount (20 wt%) the production rate drops down. This probably caused either due to excess content of mp*g*-C_3N_4 which may have filled the active sites or due to photoinduced recombination of charges. The results indicated that $CdInS_4$/20% mp*g*-C_3N_4 has a larger specific area than the compared $CdInS_4$/20% bulk-C_3N_4 because of higher active and adsorption sites. Lastly, the composite material has shown high durability, stability, and yield than others.

In David et al. (2019) and Olowoyo et al. (2019), there are many photocatalysts with different properties and performed the conversion of carbon dioxide to methanol. As per results, the reduced graphene oxide containing materials produced higher yields and excess RGO content also can contribute to lower products because of reduced graphene oxide acts as a competitor to TiO_2 in higher amounts. So, the optimisation was done and 5% of reduced graphene oxide in 5.0 RGO-TiO_2 was observed to be highest. This reaction was a success probably because of reduced graphene oxide which acted as a sensitiser of TiO_2 which increase light activity. On the whole, the experiments showed the different paths for the future of these materials used in the light-based phenomenon.

TiO_2, activated carbon fibre–TiO_2, and NiO–TiO_2/activated carbon filter were used as photocatalysts for methanol production. And the results showed that bare TiO_2 displayed

Table 2 Pollutants degradation using different photocatalysts

S. no	Photocatalytic material	Surface area ($m^2\ g^{-1}$)	Band gap energy (eV)	Pollutant degraded	Percentage degraded (%)	References
1	Sulphate-doped Ag_3PO_4	1.08	2.14	Neonicotinoid insecticide	73.66	Lee et al. (2020)
2	BiOBr/Fe_3O_4	47.38	1.75	Glyphosate	97	Cao et al. (2019)
3	Nitrogen-doped TiO_2	150	–	Iodosulphurum herbicide	74	Kralchevska et al. (2012)
4	WO_3/TiO_2	99.3	3.11	Malathion pesticide	63	Ramos-Delgado et al. (2013)
5	Zn-colayered double hydroxide composite	95.76	1.83	Gemifloxacin	60.4	Gholami et al. (2019)
6	Nanoscale cobalt aluminate	34	2.42	Navy blue textile dye	67	El Jabbar et al. (2019)
7	Zeolite-imidazole derived nanoparticles	2440	5.51	Methyl orange dye	43.3	Tran et al. (2020)
8	ZnO nanostructures	7.5	–	Sulphamethaxazole	84	Makropoulou et al. (2020)
9	MCM-41/Co_3O_4	608	1.51	Acephate pesticide	81	AbuKhadra et al. (2020)
10	g-C_3N_4/CNT/$BiVO_4$	34.99	2.70	Phenol	75	Samsudin et al. (2018)
11	Graphene quantum dots	–	–	New Fuchsin dye	100	Roushani et al. (2015)
21	CuS-CdS nanocomposite	27.11	2.2	Methylene blue dye	99	Mahanthappa et al. (2018)
12	CNTs/TiO_2/AgNPs/surfactant nanocomposites	146	2.25	Methylene blue dye	~100	Azzam et al. (2019)
13	Hydroxyl-modified titanium dioxide	129	–	Chromium	70	Li et al. (2017)
14	TiO_2@C/CdS	81.06	3.14	Chromium(VI)	96	Yin et al. (2020)
15	Calcite/TiO_2	130.33	–	Tetracycline	90.6	Belhouchet et al. (2018)
16	Bi_3TaO_7/CdS	32.87	2.98	Ciprofloxacin	27	Xu et al. (2020)
17	Heavy metal-doped titanium	–	–	Nitrobenzene	99	Nitoi et al. (2015)
18	Zinc oxide	46.149	–	Reactive blue (RB 19, RB21)	100, 91	Rodrigues et al. (2019)
19	Cerium oxide	–	–	Phenol	92.24	Ahmad et al. (2020b)
20	BN/$CdAl_2O_4$	29.60	–	Cefoxitin	–	Kumar et al. (2019c)

Ag_3PO_4 trisilver phosphate, *$BiOBr/Fe_3O_4$* bismuth oxybromide-doped ferric oxide, *TiO_2* titanium dioxide, *WO_3/TiO_2* tungsten trioxide titanium dioxide, *Zn* zinc, *ZnO* zinc oxide, *$MCM\text{-}41/Co_3O_4$* Mobil composition of matter 41 doped cobalt tetraoxide, *$g\text{-}C_3N_4/CNT/BiVO_4$* graphitic–carbon nitride-doped carbon nanotubes-modified bismuth vanadate, *CuS-CdS* copper sulphide–cadmium sulphide, *CNTs/TiO2/AgNPs* carbon nanotubes-modified titanium dioxide-doped silver nanoparticles, *TiO_2@C/CdS* titanium dioxide @ carbon-doped cadmium sulphide, *Bi_3TaO_7/CdS* bismuth tantalate-doped cadmium sulphide, *RB* reactive blue, *$BN/CdAl_2O_4$* boron nitride-doped cadmium aluminate

a lesser yield, whereas others showed higher methanol production. This increased production was seen due to immobilisations on the activated carbon fibre surfaces accompanied by electronic conductivity (Sharma and Lee 2017). NiO–TiO_2/activated carbon fibre has shown the highest product formation of the three. NiO–TiO_2/activated carbon fibre produced best results because of increased breakage of electron–hole pairs, larger surface area which supported diffusion, and enhanced effect of light shattering. The material NiO–TiO_2/activated carbon fibre was also proved to be stable and effective after 10 regenerations.

Methanol production by photocatalysis needs not be done necessarily by specific composites. A different approach to this has been performed in an experiment by Wang et al. (2016), where the pH has been considered the most crucial and pyridine catalysis has been employed. pH 5.0 was found to be optimum at a time of 6 h, whereas at pH of 4.0 and 6.0, the yield was very less because H^+ amount was not enough or in excess, respectively. The mechanism observed was pyridine and CO_2 combined to form PyCOOH via a series of proton and electron transfers. As a result, the pyridine catalysis yield has been noticed to have good results and may be used in future for fuel generations. Au/$Ti_{0.82}Si_{0.18}O_2$, Au/$Ti_{0.76}Si_{0.24}O_2$, Au/$Ti_{0.72}Si_{0.28}O_2$, Au/P25 (TiO_2) and Au/TiO_2 were used by Yadav et al. (2018) for photocatalysis. Au/$Ti_xSi_{1-x}O_2$ generated higher yields than others. And Au/$Ti_{0.72}Si_{0.28}O_2$ produced the highest compared with Au/$Ti_{0.76}Si_{0.24}O_2$ and Au/$Ti_{0.82}Si_{0.18}O_2$, and the reason for this was small nanoparticles of Au, TiO_2, and metal interaction which were proved in various results obtained from the analysis. In conclusion, the Si-doped TiO_2 was evident to be reasonable for enhanced activity.

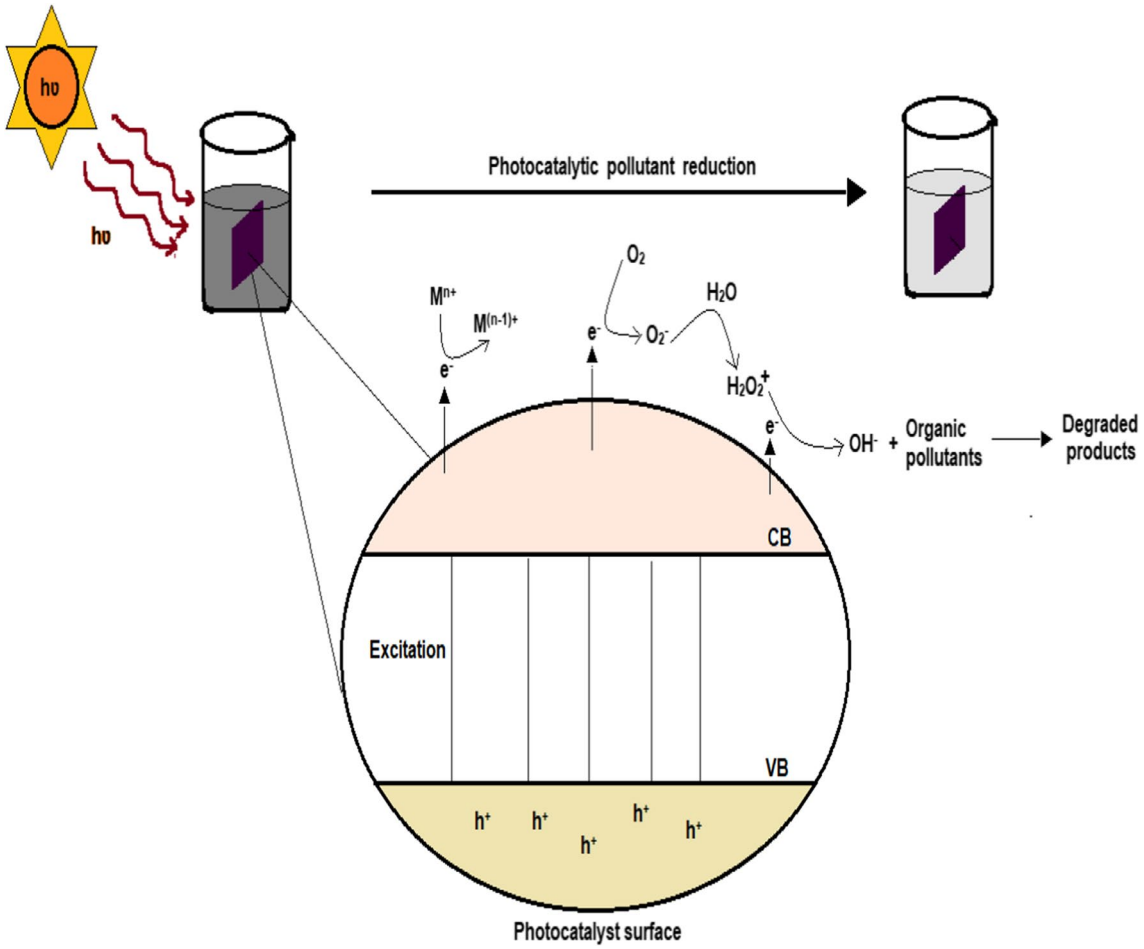

Fig. 2 Heavy metals and organic pollutants remediation by photocatalysis processes. Photocatalysis study comprises the generation of chemical energy from light energy which generates charge carriers provoking redox reactions which reduce the recalcitrant pollutants. Pollutant degradation using photocatalyst involves four major steps: mass transfer of pollutant molecules, excitation of pollutant molecules on the photocatalytic surface, degradation of pollutant molecules by oxidised compounds and desorption of decomposed compounds from photocatalytic surface to the bulk solution

Biodiesel

Owing to universal energy crisis, biodiesel has become an alternative energy source (Roslindawati et al. 2017). For the biodiesel production, novel photocatalytic materials have been utilised in trans-esterification of substrates. Novel CaO/TiO_2 (calcium oxide-titanium dioxide) catalysts was prepared by photochemical mechanism and utilised for the production of biodiesel from microalgal biomass. Biodiesel production was performed in a reactor with methanol and *Chlorella vulgaris* biomass powder for 1 h at a fixed pressure range. Significant compounds such as fatty acid methyl esters were observed to be present in the resultant analysis, and the biodiesel yield was increased to around 51.6% (Aghilinategh et al. 2019). Another study was explored using ZnO/SiO_2 catalyst with *Jatropha Curcas* crude oil as substrate. Broadly, the biodiesel generation involves two primary steps: free fatty acid photo-esterification and alkali catalysed trans-esterification. In the first step, photocatalytic experiments were performed in a ultraviolet photoreactor with optimal reaction conditions. The mechanism of photocatalytic trans-esterification process is as follows: free fatty acids and methanol transfer and adsorption from the solution to the photocatalyst surface, adsorbed phase reaction such as redox reactions to form radicals, formation of fatty acid esters, desorption of the formed esters and their corresponding transfer to the liquid phase. The synthesised photocatalyst used was efficient and reusable for around 10 biodiesel production cycles. The process infers the heterogenic photocatalysis nature of biodiesel production (Corro et al. 2013). Another photocatalysts such as Cr/SiO_2 and $TiCl_2$ photocatalysts were employed for the trans-esterification process for biodiesel production. In the former catalyst, existence of chromium ion groups assists in the absorption of photons

and generation of electron–hole pairs thus performing trans-esterification and photo-esterification of methanol. Extraction of lipids from *Nannochloropsis* was carried out using photocatalysis process. Consecutively, reactive oxygen species are produced which disrupts the cell membrane releasing lipids. The generated radicals were further used for trans-esterification of the lipids. Gas chromatography mass spectrometry (GCMS) analysis inferred the presence of benzene methanol, cyclohexane, etc. (Corro et al. 2017; Shwetharani and Balakrishna 2016). Thus the above studies confirm the efficiency of photocatalysts for biodiesel production. However, studies have to be explored for improving the efficiency of the photocatalysts for biofuel production.

Hydrogen

Hydrogen is a zero-emission fuel, which has been used in vehicles for many years. It has been produced using various methods, either from fossil fuels, by steam methane reforming or gasification or electrolysis processes, or by solar fuel cells. It is sometimes hazardous because it has low ignition and high combustion energies, so, it may leak from the container. In Sun et al. (2020a), bare Cu_2O, pure CZTS (Cu_2ZnSnS_4), CZTS/Cu_2O-1, CZTS/Cu_2O-2, and CZTS/Cu_2O-3 have been compared for photocatalytic hydrogen production. As per the results, bare Cu_2O has a negligible amount of hydrogen yield, whereas bare CZTS generated higher production rates. The synergistic effect of CZTS and Cu_2O increased the yield relatively. CZTS/Cu_2O-2 had maximum hydrogen generation, which was 7.7 times greater than the CZTS result. CZTS/Cu_2O-2 was tested based on its stability, and analysis disclosed that they were highly stable and efficient. Hydrogen generation can be done with the help of methanol/glycerol using the photocatalysts TiO_2, Pt/TiO_2, 1% CNT–Pt/TiO_2 (C–TiO_2/g-C_3N_4), 5% CNT–Pt/TiO_2, 10% CNT–Pt/TiO_2 and 20% CNT–Pt/TiO_2 (Naffati et al. 2020). The carbon naotube-TiO_2 hybrids were more effective than Pt–TiO_2, because of enhanced photo-efficiency in the composites. And the highest yield was obtained by 1% CNT–Pt/TiO_2 with 2327 and 2019 µmol g^{-1} using methanol and glycerol, respectively. However, more than 1% carbon nanotubes composites showed decreased hydrogen evolution and 20% showed the lowest yield. Thus, the study shows that when the carbon nanotube content is too high, the light penetration becomes difficult, and it is important to know the optimum amount required for higher production.

TiO_2 coupled with g-C_3N_4 has been utilised as photocatalysts for the production of hydrogen (Han et al. 2019). The amount of hydrogen evolution is highest for C-Ti/CN-10, where it clearly indicates that more than bare C–TiO_2. The photocatalytic activity of C–TiO_2 and g-C_3N_4 was 24 and 8 times lower than that of C–TiO_2/g-C_3N_4 composites. In Nagajyothi et al. (2020)'s work, the $ZnFe_2O_4$ and MoS_2 were two materials that were combined to form an effective catalyst. And the findings showed that 2-ZFO/MS/Pt-10 ($ZnFeO_4$/MoS_2) had the highest yield, and the next after which was 2-ZFO/MS/Pt-15 followed by 2-ZFO/MS/Pt-5. The hybrid's performance was justified by the following reasons, large surface area, quicker electron transfers, co-catalyst interactions with water, redox activity of Zn and Fe ions, and separation potentials of the combinations used. In this study also, it is exhibited that the hybrids or composites have more efficiency than the pure and they enhance the stability of the material used for hydrogen generation.

Janus nanofibre heterojunction photocatalyst (JNHP), T-NP, B-NP, M-NP (TiO_2/C, Bi_2WO_6/C) were analysed in the experiment by Sun et al. (2020b). JNHP-2 was observed to have the highest yield of hydrogen, and M-NP was lower which is described by the fact that B-NP and T-NP are not completely fused. Consecutive rounds of photocatalysis were carried to check the quality of JNHP-2, and the results showed that the photocatalyst had good stability, flexibility, and other properties. In a wavelength of $320 \leq \lambda \leq 780$ nm, JNHP produced more yield than in $420 \leq \lambda \leq 780$ nm that is 16.32 mmol $h^{-}1$ g^{-1}. Furthermore, there was no usage of metals as cocatalyst in this process. 1Pt–TiO_2-2 and TiO_2-2–1Pt have been compared with TiO_2 in Chung et al. (2019) and the results showed that the combinations used produced good outputs, but it cannot be clearly explained which of the combinations is more preferred. Also, when NaOH was used, the investigation of the procedure exposed that the addition of the base decreased the photocatalytic activity, which moreover led to the conclusion that it is better to include washing step for higher hydrogen yield. In another study (Gil et al. 2020), ZnS–ZnO/ZnAl-LDH composites were used in different proportions, i.e. ZA-S1, ZA-S2, ZA-S3, and ZA-S4. Sulphur ions and ZA material were proven to be responsible for a higher hydrogen yield rate. But the excess sulphur presence lowered the yield as well. Among the hybrids, ZA-S3 produced the highest amount of hydrogen, followed by ZA-S4, ZA-S2, and ZA-S1. Only ZA did not produce any hydrogen because of the large bandgap of ZnAl-LDH.

Sm-doped ZnO/g-C_3N_4 composites have been used by Rakibuddin and Kim (2020) in various combinations like SAZOC-5, SAZOC-10 and SAZOC-15. After the analysis, SAZOC 10 was observed having the largest hydrogen evolution then SAZOC 15, SAZOC 5, g-C_3N_4, and Sm-ZnO. While stability testing, there was no decrease in the hydrogen production rate until 8 h. After 8 h, due to leaching, there was a small reduction in hydrogen reduction. Overall, the material SAZOC10 had good stability and photocatalytic properties. In Shahzad et al. (2019b), WO_3, WO_3/4% fullerene, WO_3–/0.5% fullerene, Ni_3B/Ni $(OH)_2$ and WO_3/2% fullerene Ni_3B/Ni $(OH)_2$ were represented by S1, S2, S3, S4, S5 and S6, respectively. And the highest evolution of H_2 was

seen in S5 followed by S6 than S4, S3, S2 and S1. After stability testing, the results collected showed that S5 was highly efficient and reusable and doping indeed helps in increasing the yield of hydrogen and separation characteristics. M–M (mechanical mixing) Er^{3+}: $Y_3Al_5O_{12}$@Nb_2O_5/In_2O_3, C–D (coating-demolding) Er^{3+}: $Y_3Al_5O_{12}$@ Nb_2O_5/In_2O_3 and C-D Er^{3+}: $Y_3Al_5O_{12}$@ Nb_2O_5/Pt/In_2O_3 were prepared for Z scheme photocatalysis (Xing et al. 2020). The two C–D schemes had a higher production rate than the M–M scheme. The differences in the scheme were due to Pt conducted between Nb05 and In_2O_3 and makes electron's faster transfer to valence band. Pure TiO_2 NPs and Au/TiO_2 composites were compared in a recent study (Wang et al. 2020). The different composites used were 0.1 g/L Au/TiO_2, 0.5 g/L Au/TiO_2, 1 g/L Au/TiO_2. The various yields produced were examined and the results were 1 g/L Au/TiO_2 > 0.5 g/L Au/TiO_2 > 0.1 g/L Au/TiO_2 > pure TiO_2. On the whole, the noble metal material produced 1 g/L Au/TiO_2 exhibited the highest yield. Cl-Ta_2O_5-x microspheres were taken by Yu et al. (2020) for performing photocatalytic hydrogen generation. The microspheres arrest the light, inside them and then generate hydrogen. Among the microspheres used, Cl-Ta_2O_5-x-200 shows significantly higher stability. The content of hydrogen evolutions tended to increase when the number of microspheres was increased from the methanol solution. Finally, the other analysis results were obtained and the material was proved to be stable photocatalyst. Photocatalytic hydrogen generation by MoO_3@MoS_2/TiO_2 was performed by Zhang et al. (2019c). The same composites were used at different temperature using M-10T i.e. M-310T (at 310 °C), M-320T (at 320 °C), M-330T (at 330 °C), M-340T (at 340 °C), M-350T (at 350 °C), and M-360T (at 360 ° C) along with 1.3 montmorillonite and TiO_2 for comparison. The quenching temperature was decreased which further resulted in the increase in yield from 2234 to 4691 µmol h^{-1} g^{-1}. Hydrogen yield of distinct photocatalysts used for hydrogen production is shown in Table 3. In conclusion, the quenching method was established to be advantageous and it also increases sites of adsorption and efficiency. Biofuel production by the photocatalysts is shown in Fig. 3.

Limitations

Even though photocatalysis has many advantages, there are an equal number of challenges which makes the current photocatalysis as a less usable option. When it comes to materials used in photocatalysis, the material must be suitable for photocatalysis in all possible ways. But there are only limited ones which can be used because many lack any one main factor. For example, semiconductors with sulphides, oxides, or nitrides can be used for photocatalysis, but some have a small range for absorption and others are not stable in the aqueous medium (Mishra and Chun 2015). Metal oxides have been used as photocatalyst widely too, but they also have some disadvantages like less adsorption, lower recovery, less reusability and higher recombination rates (Mohamed et al. 2020). TiO_2-based elements have been widely used for photocatalysis, and they have many advantages. However, they show poor performance when used alone, and they also possess comparatively less oxygen production, fast recombination rate, and poor charge transportation. Another problem is that the ultraviolet with high energy band entering the earth is already less and TiO_2 requires very high energy to get activated. Hence, the productivity of TiO_2 is reduced (Adekoya et al. 2017). It is also said to have lower quantum yield, less adsorption potential, and surface area (Lum et al. 2019). Similarly, ZnO also has lower adsorption potential and is non-porous. ZnO is very unstable in both alkaline and acidic conditions and gets accumulated to bulk easily.

When there is the use of microbes while fuel generation, the challenges increase because of many reasons. One of them is by-products; this can be a major problem when we want to extract particular gas, e.g. hydrogen, and the extra product, e.g. carbon dioxide. This can make the process tedious and difficult. Also, the residues produced may influence product production as microbial pathways can be influenced by various factors. For these types of problems, the need for newer and better reactors and engineered microbes are required. Water-splitting processes have been used along with photocatalysis to extract hydrogen. Alsayegh et al. (2018) have explained the challenges that are faced while this process briefly. When hydrogen and oxygen are separated physically using a reactor, there is a consequence of explosion along with the recovery process which is costly and tedious.

Although the nano-photocatalysts are proven to be highly efficient, some challenges limit their usage too, Chen et al. (2019) have highlighted the same. Inorganic nano-photocatalysts have lower charge transport and organic possess weak interactions. Moreover, the heterostructures should be studied in-depth and their function in the catalysis should also be identified for better results. After the quantitative and qualitative prediction of the material, we can be able to use this for pollutant removals or fuel generation in industrial scales. Other problems with nanoparticles (Mamba et al. 2019) are the accumulation of photocatalysts, low recovery rates and metal leaching. Even though there have been many solutions that are emerging, the requirement of metal-free or low metal catalysts that are less hazardous is always present. When we take an industrial perspective into account, the cost, efficiency and life of the material can majorly affect the product. The price always matters when quantity increases, so a cheap catalyst is the primary aim, but many photocatalysts are either doped or mixed with elements like

Table 3 Hydrogen yield of different photocatalysts used for hydrogen production

S. no.	Photocatalytic material	BET surface area ($m^2\ g^{-1}$)	Hydrogen yield ($\mu mol\ h^{-1}\ g^{-1}$)	References
1	Hydrophilic poloxamer-coated $SrTiO_3$	48.51	402	Zhu et al. (2020)
2	CZTS/Cu_2O-2	–	897.23	Sun et al. (2020a)
3	CNT-TiO_2- 1%	11	2327	Naffati et al. (2020)
4	C–TiO_2/*g*-C_3N_4-10	129.6	1409	Han et al. (2019)
5	2-ZFO/MS/Pt-10	57.84	1973.57	Nagajyothi et al. (2020)
6	JNHP-2	–	11,580	Sun et al. (2020b)
7	ZA-S3	78	1599	Gil et al. (2020)
8	SAZOC 10	–	10.25	Rakibuddin and Kim (2020)
9	S5(WO_3/2% fullerene Ni_3B/Ni $(OH)_2$)	495.76	~ 1600	Shahzad et al. (2019b)
10	MoS_2(340 °C)/TiO_2	30.6	4669	Zhang et al. (2019c)
11	TiO_2-PtFAC (TiO_2 catalyst with facet exposure loaded with platinum	70	~13,000	Vaiano et al. (2018)
12	AgNPs/*g*-C_3N_4	139	152.2	Liu et al. (2018)
13	CdS/*g*-C_3N_4	–	83	Liu et al. (2015)
14	*g*-C_3N_4/CB/NiS	83.68	992	Wen et al. (2015)
15	S-doped and N deficient *g*-C_3N_4	72.8	121	Chen et al. (2015)
16	MoS_2/TiO_2	167	5424	Xie et al. (2020)
17	NiO/TiO_2 supported carbon nanosheets	81	1.55	Zhao et al. (2020)
18	*g*-C_3N_4/TiO_2	152–176	1041	Alcudia-Ramos et al. (2019)
19	Carbon-doped $KNbO_3$	1.3	211	Yu et al. (2018)
20	NiS/graphite nitride/Strontium titanate composites	37.4	1722	Luo et al. (2018)
21	TiO_2/MoS_2/Au-Cu ternary hybrid	34.28	750	Liu et al. (2019)
22	Bismuth–metal organic framework (Bi-TBAPy)	594	140	Xiao et al. (2019)

$SrTiO_3$ strontium titanate, *CZTS/Cu_2O* copper zinc tin sulphide/cuprous oxide, *CNT-TiO_2* carbon nanotubes-doped titanium dioxide, *C–TiO_2/g-C_3N_4* carbon-modified titanium dioxide-doped graphitic carbon nitrides, *ZFO/MS/Pt* zinc ferrite molybdenum sulphide-doped platinum, *JNHP* janus nanofibre heterojunction photocatalyst, *ZA* Z L aspartic acid, *SAZOC* samarium-doped zinc oxide coupled, *MoS_2* molybdenum sulphide, *TiO_2* titanium dioxide, *TiO_2-PtFAC* titanium dioxide- facet exposure loaded with platinum, *AgNPs/g-C_3N_4* silver nanoparticles-doped graphitic carbon nitrides, *CdS/g-C_3N_4* cadmium sulphide-doped graphitic carbon nitrides, *g-C_3N_4/CB/NiS* graphitic carbon nitrides carbon black-doped nickel sulphide, *g-C_3N_4* graphitic carbon nitrides, *NiO* nickel oxide, *g-C_3N_4/TiO_2* graphitic carbon nitrides-doped titanium dioxide, *$KNbO_3$* potassium niobate, *NiS* nickel sulphide, *TiO_2/MoS_2/Au-Cu* titanium dioxide-doped molybdenum disulphide gold-copper, *Bi-TBAPy* bismuth organic framework

gold (Yadav et al. 2018) and platinum (Chung et al. 2019) which not only increases the efficiency but also increases the cost. And the combined materials used become harder to study and also adds money to the process. Additionally, the photocatalyst is used in large scales for fuel generation, therefore are supposed to have higher life. But, most of the photocatalysts are only efficient for 2–3 cycles, after which the fuel production reduces. Hence, these limitations have to be overcome in further explications.

Conclusion

Photocatalytic systems for the remediation of environmental pollutants have been exemplified as an efficient technique from various research studies. Currently, novel photocatalysts have been developed and used for the pollutant removal, but the cost of the material synthesis has to be minimised by further studies. The wide range of usage in removal of persistent organic pollutants such as antibiotics, pesticides and herbicides was noted with novel photocatalysts developed. Though energy generation using photocatalytic processes was found to be effective, production of by-products along with the main product limits their efficiency. The development of biofuel has emerged in recent years making microbial species as essential substrate along with photocatalyst for biofuel production. Microbial pathways influence the photocatalytic mechanism which has to be explored in future researches. Most of the photocatalysts are developed from metals which may further lead to polluted environment. Hence the alternative environment friendly photocatalytic materials have to be developed to mitigate the ecological effects. Also future explications in photocatalytic removal of environmental pollutants should focus on the optimising reaction parameters using mathematical modelling.

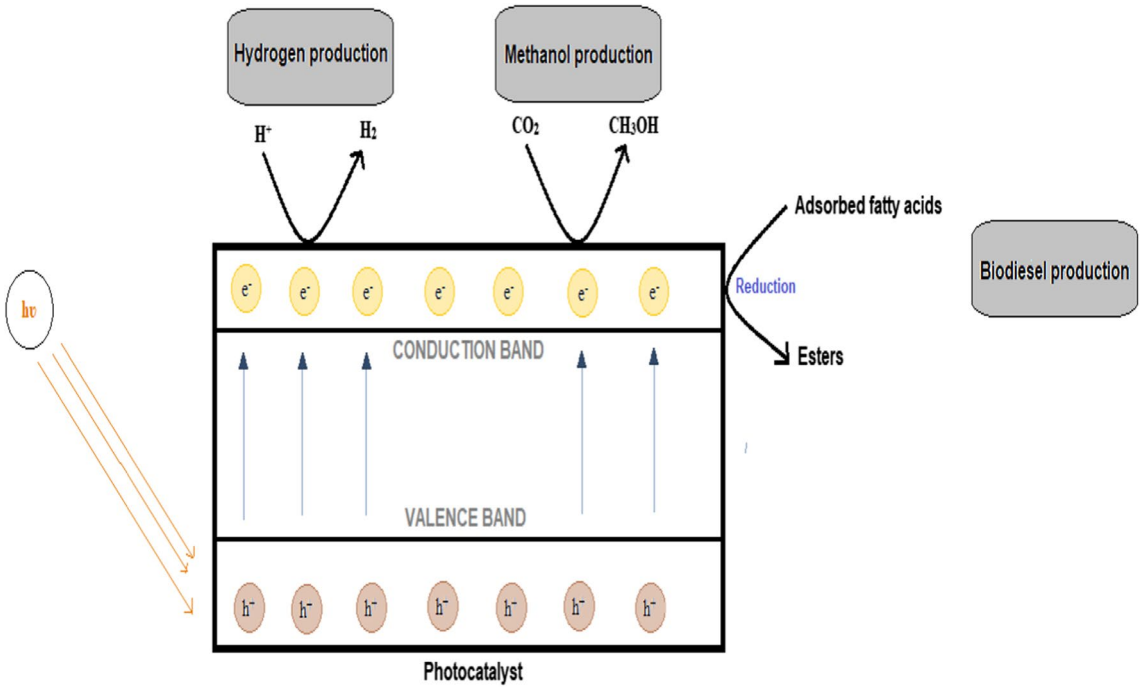

Fig. 3 Biofuel production by photocatalysis. The photocatalytic improving of aqueous solution of biomass could be an intriguing and imaginative course to create hydrogen in encompassing conditions. The development of biofuel has emerged in recent years making microbial species as essential substrate along with photocatalyst for biofuel production

References

Abdennouri M, Elhalil A, Farnane M, Tounsadi H, Mahjoubi FZ, Elmoubarki R, Sadiq M, Khamar L, Galadi A, Baalala M, Bensitel M, El-hafiane Y, Smith A, Barka N (2015) Photocatalytic degradation of 2,4-D and 2,4-DP herbicides on Pt/TiO_2 nanoparticles. J Saudi Chem Soc 19(5):485–493. https://doi.org/10.1016/j.jscs.2015.06.007

AbuKhadra MR, Mohamed AS, El-Sherbeeny AM, Elmeligy MA (2020) Enhanced photocatalytic degradation of acephate pesticide over MCM-41/Co_3O_4 nanocomposite synthesized from rice husk silica gel and Peach leaves. J Hazard Mater 389:122129. https://doi.org/10.1016/j.jhazmat.2020.122129

Adekoya DO, Tahir M, Amin NAS (2017) g-C_3 N_4/(Cu/TiO_2) nanocomposite for enhanced photoreduction of CO_2 to CH_3 OH and HCOOH under UV/visible light. J CO2 Util 18:261–274. https://doi.org/10.1016/j.jcou.2017.02.004

Aghilinategh M, Barati M, Hamadanian M (2019) Supercritical methanol for one put biodiesel production from chlorella vulgaris microalgae in the presence of CaO/TiO_2 nano-photocatalyst and subcritical water. Biomass Bioenerg 123:34–40. https://doi.org/10.1016/j.biombioe.2019.02.011

Ahamad T, Naushad M, Al-Saeedi SI, Almotairi S, Alshehri SM (2019) Fabrication of MoS_2/ZnS embedded in N/S doped carbon for the photocatalytic degradation of pesticide. Mater Lett. https://doi.org/10.1016/j.matlet.2019.127271

Ahmad K, Ghatak HR, Ahuja SM (2020a) Photocatalytic technology: a review of environmental protection and renewable energy application for sustainable development. Environ Technol Innov 19:100893. https://doi.org/10.1016/j.eti.2020.100893

Ahmad T, Iqbal J, Bustam MA, Zulfiqar M, Muhammad N, Al Hajeri BM, Irfan M, Anwaar Asghar HM, Ullah S (2020b) Phytosynthesis of cerium oxide nanoparticles and investigation of their photocatalytic potential for degradation of phenol under visible light. J Mol Struc 1217:128292. https://doi.org/10.1016/j.molstruc.2020.128292

Alcudia-Ramos MA, Fuentez-Torres MO, Ortiz-Chi F, Espinosa-González CG, Hernández-Como N, García-Zaleta DS, Kesarla MK, Torres-Torres JG, Collins-Martinez V, Godavarthi S (2019) Fabrication of g-C_3N_4/TiO_2 heterojunction composite for enhanced photocatalytic hydrogen production. Ceram Int 46:38–45. https://doi.org/10.1016/j.ceramint.2019.08.228

Al-Hamdi AM, Sillanpää M, Bora T, Dutta J (2016) Efficient photocatalytic degradation of phenol in aqueous solution by SnO_2: Sb nanoparticles. Appl Surf Sci 370:229–236. https://doi.org/10.1016/j.apsusc.2016.02.123

Alsayegh S, Johnson JR, Ohs B, Wessling M (2018) Methanol production via direct carbon dioxide hydrogenation using hydrogen from photocatalytic water splitting: process development and techno-economic analysis. J Clean Prod 208:1446–1458. https://doi.org/10.1016/j.jclepro.2018.10.132

Amalraj A, Pius A (2015) Photocatalytic degradation of monocrotophos and chlorpyrifos in aqueous solution using TiO_2 under UV radiation. J Water Process Eng 7:94–101. https://doi.org/10.1016/j.jwpe.2015.06.002

Anandan S, Kumar Ponnusamy V, Ashokkumar M (2020) A review on hybrid techniques for the degradation of organic pollutants in aqueous environment. Ultrason Sonochem 67:105130. https://doi.org/10.1016/j.ultsonch.2020.10513

Anitha T, Kumar PS, Kumar KS (2015) Binding of Zn (II) ions to chitosan–PVA blend in aqueous environment: adsorption kinetics

and equilibrium studies. Environ Prog Sustain Energy 34:15–22. https://doi.org/10.1002/ep.11943

Ayodhya D, Veerabhadram G (2018) A review on recent advances in photodegradation of dyes using doped and heterojunction based semiconductor metal sulfide nanostructures for environmental protection. Mater Today Energy 9:83–113. https://doi.org/10.1016/j.mtener.2018.05.007

Ayodhya D, Veerabhadram G (2019) Fabrication of Schiff base coordinated ZnS nanoparticles for enhanced photocatalytic degradation of chlorpyrifos pesticide and detection of heavy metal ions. J Materiomics 5:446–454. https://doi.org/10.1016/j.jmat.2019.02.002

Azzam EMS, Fathy NA, El-Khouly SM, Sami RM (2019) Enhancement the photocatalytic degradation of methylene blue dye using fabricated CNTs/TiO_2/AgNPs/Surfactant nanocomposites. J Water Process Eng 28:311–321. https://doi.org/10.1016/j.jwpe.2019.02.016

Babić S, Ćurković L, Ljubas D, Čizmić M (2017) TiO_2 assisted photocatalytic degradation of macrolide antibiotics. Curr Opin Green Sustain Chemi 6:34–41. https://doi.org/10.1016/j.cogsc.2017.05.004

Belhouchet N, Hamdi B, Chenchouni H, Bessekhouad Y (2018) Photocatalytic degradation of tetracycline antibiotic using new calcite/titania nanocomposites. J Photochem Photobiol, A 372:196–205. https://doi.org/10.1016/j.jphotochem.2018.12.016

Belver C, Bedia J, Gómez-Avilés A, Peñas-Garzón M, Rodriguez JJ (2019) Semiconductor photocatalysis for water purification. In: Thomas S (ed) Nanoscale materials in water purification. Elsevier, Amsterdam, pp 581–651. https://doi.org/10.1016/B978-0-12-813926-4.00028-8

Cao L, Ma D, Zhou Z, Xu C, Cao C, Zhao P, Huang Q (2019) Efficient photocatalytic degradation of herbicide glyphosate in water by magnetically separable and recyclable BiOBr/Fe_3O_4 nanocomposites under visible light irradiation. Chem Eng J 368:212–222. https://doi.org/10.1016/j.cej.2019.02.100

Chen J, Hong Z, Chen Y, Lin B, Gao B (2015) One-step synthesis of sulfur-doped and nitrogen-deficient g-C_3N_4 photocatalyst for enhanced hydrogen evolution under visible light. Mater Lett 145:129–132. https://doi.org/10.1016/j.matlet.2015.01.073

Chen Y, Jiang D, Gong Z, Li Q, Shi R, Yang Z, Lei Z, Li J, Wang L-N (2019) Visible-light responsive organic nano-heterostructured photocatalysts for environmental remediation and H_2 generation. J Mater Sci Technol 38:93–106. https://doi.org/10.1016/j.jmst.2019.09.003

Chen L, Wang X, Chen Y, Zhuang Z, Chen F-F, Zhu Y-J, Yu Y (2020) Recycling heavy metals from wastewater for photocatalytic CO_2 reduction. Chem Eng J 402:125922. https://doi.org/10.1016/j.cej.2020.125922

Cheng M, Zeng G, Huang D, Lai C, Liu Y, Xu P, Zhang C, Wan J, Hu L, Xiong W, Zhou C (2017) Salicylic acid–methanol modified steel converter slag as heterogeneous Fenton-like catalyst for enhanced degradation of alachlor. Chem Eng J 327:686–693. https://doi.org/10.1016/j.cej.2017.06.153

Chung Y-H, Han K, Lin C-Y, O'Neill D, Mul G, Mei B, Yang C-M (2019) Photocatalytic hydrogen production by photo-reforming of methanol with one-pot synthesized Pt-containing TiO_2 photocatalysts. Catal Today. https://doi.org/10.1016/j.cattod.2019.07.042

Corro G, Pal U, Tellez N (2013) Biodiesel production from Jatropha curcas crude oil using ZnO/SiO_2 photocatalyst for free fatty acids esterification. Appl Catal B 129:39–47. https://doi.org/10.1016/j.apcatb.2012.09.004

Corro G, Sánchez N, Pal U, Cebada S, Fierro JLG (2017) Solar-irradiation driven biodiesel production using Cr/SiO_2 photocatalyst exploiting cooperative interaction between Cr_{6+} and Cr_{3+} moieties. Appl Catal B 203:43–52. https://doi.org/10.1016/j.apcatb.2016.10.005

David A, Muhammad T, Amin Nor Aishah Saidina (2019) Recent trends in photocatalytic materials for reduction of carbon dioxide to methanol. Renew Sust Energy Rev 116:109389. https://doi.org/10.1016/j.rser.2019.109389

Dewidar H, Nosier SA, El-Shazly AH (2018) Photocatalytic degradation of phenol solution using zinc oxide/UV. J Chem Health Saf 25(1):2–11. https://doi.org/10.1016/j.jchas.2017.06.001

Dhandole LK, Kim S-G, Bae H-S, Ryu HI, Chung H-S, Seo Y-S, Cho M, Shea PJ, Jang JS (2019) Simultaneous and synergistic effect of heavy metal adsorption on the enhanced photocatalytic performance of a visible-light-driven RS-TONR/TNT composite. Environ Res 180:108651. https://doi.org/10.1016/j.envres.2019.108651

Di Paola A, García-López E, Marcì G, Palmisano L (2012) A survey of photocatalytic materials for environmental remediation. J Hazard Mater 211–212:3–29. https://doi.org/10.1016/j.jhazmat.2011.11.050

Diao Z-H, Xu X-R, Liu F-M, Sun Y-X, Zhang Z-W, Sun K-F, Wang S-Z, Cheng H (2015) Photocatalytic degradation of malachite green by pyrite and its synergism with Cr(VI) reduction: performance and reaction mechanism. Sep Purif Technol 154:168–175. https://doi.org/10.1016/j.seppur.2015.09.027

Dileepkumar VG, Surya PS, Pratapkumar C, Viswanatha R, Ravikumar CR, Anil Kumar MR, Muralidhara HB, Al-Akraa IM, Mohammad AM, Chen Z, Bui X-T, Santosh MS (2020) $NaFeS_2$ as a new photocatalytic material for the degradation of industrial dyes. J Environ Chem Eng 8(4):104005. https://doi.org/10.1016/j.jece.2020.104005

Do TCMV, Nguyen DQ, Nguyen KT, Le PH (2019) TiO_2 and Au-TiO_2 nanomaterials for rapid photocatalytic degradation of antibiotic residues in aquaculture wastewater. Materials 12(15):2434. https://doi.org/10.3390/ma12152434

Dong S, Cui L, Zhang W, Xia L, Zhou S, Russell CK, Fan M, Feng J, Sun J (2019) Double-shelled $ZnSnO_3$ hollow cubes for efficient photocatalytic degradation of antibiotic wastewater. Chem Eng J 384:123279. https://doi.org/10.1016/j.cej.2019.123279

Eckert H, Bobeth M, Teixeira S, Kühn K, Cuniberti G (2015) Modeling of photocatalytic degradation of organic components in water by nanoparticle suspension. Chem Eng J 26:67–75. https://doi.org/10.1016/j.cej.2014.05.147

El Jabbar Y, El Hafdi M, Benchikhi M, El Ouatib R, Er-Rakho L, Essadki A (2019) Photocatalytic degradation of navy blue textile dye by nanoscale cobalt aluminate prepared by polymeric precursor method. Environ Nanotechnol Monit Manage 12:100259. https://doi.org/10.1016/j.enmm.2019.100259

Ganguly P, Panneri S, Hareesh US, Breen A, Pillai SC (2019) Recent Advances in Photocatalytic detoxification of water. In: Thomas S (ed) Nanoscale materials in water purification. Elsevier, Amsterdam, pp 653–688. https://doi.org/10.1016/B978-0-12-813926-4.00029-X

Gholami P, Khataee A, Soltani RDC, Dinpazhoh L, Bhatnagar A (2019) Photocatalytic degradation of gemifloxacin antibiotic using Zn-Co-LDH@biochar nanocomposite. J Hazard Mater 382:121070. https://doi.org/10.1016/j.jhazmat.2019.121070

Gil JJ, Aguilar-Martínez O, Piña-Pérez Y, Pérez-Hernández R, Santolalla-Vargas CE, Gómez R, Tzompantzi F (2020) Efficient ZnS–ZnO/ZnAl-LDH composite for H_2 production by photocatalysis. Renew Energy 145:124–132. https://doi.org/10.1016/j.renene.2019.06.001

Gusain R, Gupta K, Joshi P, Khatri OP (2019) Adsorptive removal and photocatalytic degradation of organic pollutants using metal oxides and their composites: a comprehensive review. Adv Colloid Interface Sci 272:102009. https://doi.org/10.1016/j.cis.2019.102009

Hakobyan K, Gegenhuber T, McErlean CS, Müllner M (2019) Visible-light-driven MADIX polymerisation via a reusable, low-cost, and non-toxic bismuth oxide photocatalyst. Angew Chem Int Ed 58:1828–1832

Han X, An L, Hu Y, Li Y, Hou C, Wang H, Zhang Q (2019) Ti_3C_2 MXene-derived carbon-doped TiO_2 coupled with g-C_3N_4 as the visible-light photocatalysts for photocatalytic H_2 generation. Appl Catal B 265:118539. https://doi.org/10.1016/j.apcatb.2019.118539

Hasanpour M, Hatami M (2020) Photocatalytic performance of aerogels for organic dyes removal from wastewaters: review study. J Mol Liq 309:113094. https://doi.org/10.1016/j.molliq.2020.113094

Helal A, Harraz FA, Ismail AA, Sami TM, Ibrahim I (2017) Hydrothermal synthesis of novel heterostructured Fe_2O_3/Bi_2S_3 nanorods with enhanced photocatalytic activity under visible light. Appl Catal B 213:18–27. https://doi.org/10.1016/j.apcatb.2017.05.009

Hitam CNC, Jalil AA (2020) A review on exploration of Fe_2O_3 photocatalyst towards degradation of dyes and organic contaminants. J Environ Manag 258:110050. https://doi.org/10.1016/j.jenvman.2019.110050

Huang D, Chen S, Zeng G, Gong X, Zhou C, Cheng M, Xue W, Yan X, Li J (2019) Artificial Z-scheme photocatalytic system: what have been done and where to go? Coord Chem Rev 385:44–80. https://doi.org/10.1016/j.ccr.2018.12.013

Jeevanantham S, Saravanan A, Hemavathy RV, Kumar PS, Yaashikaa PR, Yuvaraj D (2019) Removal of toxic pollutants from water environment by phytoremediation: a survey on application and future prospects. Environ Technol Innov 13:246–276. https://doi.org/10.1016/j.eti.2018.12.007

Juan Y, Jingyi H, Jianping W, Jun D, Yao L (2020) Visible-light-driven selective oxidation of methane to methanol on amorphous FeOOH coupled m-WO_3. Fuel 266:117104. https://doi.org/10.1016/j.fuel.2020.117104

Kanan S, Moyet MA, Arthur RB, Patterson HH (2019) Recent advances on TiO_2-based photocatalysts toward the degradation of pesticides and major organic pollutants from water bodies. Catal Rev 62(3):1–65. https://doi.org/10.1080/01614940.2019.1613323

Kangralkar MV, Kangralkar VA, Momin N, Manjanna J (2019) Cu_2O nanoparticles for removal of methylene blue dye from solution. Environ Nanotechnol Monit Manag 12:100265. https://doi.org/10.1016/j.enmm.2019.100265

Khan SH, Pathak B (2020) Zinc oxide based photocatalytic degradation of persistent pesticides: a comprehensive review. Environ Nanotechnol Monit Manag 10:100290. https://doi.org/10.1016/j.enmm.2020.100290

Kiruba UP, Kumar PS, Prabhakaran C, Aditya V (2014) Characteristics of thermodynamic, isotherm, kinetic, mechanism and design equations for the analysis of adsorption in Cd(II) ions-surface modified Eucalyptus seeds system. J Taiwan Inst Chem Eng 45:2957–2968. https://doi.org/10.1016/j.jtice.2014.08.016

Konstantinou IK, Sakellarides TM, Sakkas VA, Albanis TA (2001) Photocatalytic degradation of selected s-Triazine herbicides and organophosphorus insecticides over aqueous TiO_2 suspensions. Environ Sci Technol 35(2):398–405. https://doi.org/10.1021/es001271c

Kralchevska R, Milanova M, Tišler T, Pintar A, Tyuliev G, Todorovsky D (2012) Photocatalytic degradation of the herbicide iodosulfuron by neodymium or nitrogen doped TiO_2. Mater Chem Phys 133:1116–1126. https://doi.org/10.1016/j.matchemphys.2012.02.025

Kumar A, Kumar Prajapati P, Aathira MS, Bansiwal A, Boukherroub R, Jain SL (2019a) Highly improved photoreduction of carbon dioxide to methanol using cobalt phthalocyanine grafted to graphitic carbon nitride as photocatalyst under visible light irradiation. J Colloid Interface Sci 543:201–213. https://doi.org/10.1016/j.jcis.2019.02.061

Kumar B, Bhardwaj N, Verma P (2019b) Pretreatment of rice straw using microwave assisted $FeCl_3$-H_3PO_4 system for ethanol and oligosaccharides generation. Bioresour Technol Rep 7:100295. https://doi.org/10.1016/j.biteb.2019.100295

Kumar R, Barakat MA, Al-Mur BA, Alseroury FA, Eniola JO (2019c) Photocatalytic degradation of cefoxitin sodium antibiotic using novel BN/$CdAl_2O_4$ composite. J Clean Prod 246:119076. https://doi.org/10.1016/j.jclepro.2019.119076

Lee SC, Jeong Y, Kim YJ, Kim H, Lee HU, Lee Y-C, Lee SM, Kim HJ, Lee G-W, Lee Y-S, Lee G (2018) Hierarchically three-dimensional (3D) nanotubular sea urchin-shaped iron oxide and its application in heavy metal removal and solar-induced photocatalytic degradation. J Hazard Mater 354:283–292. https://doi.org/10.1016/j.jhazmat.2018.04.048

Lee B-H, Park S, Kim M, Sinha AK, Lee SC, Jung E, Chang WJ, Lee K-S, Kim JH, Cho S-P (2019) Reversible and cooperative photoactivation of single-atom Cu/TiO_2 photocatalysts. Nat Mater 18:620–626. https://doi.org/10.1038/s41563-019-0344-1

Lee Y-J, Kang J-K, Park S-J, Lee C-G, Moon J-K, Alvarez PJJ (2020) Photocatalytic degradation of neonicotinoid insecticides using sulfate-doped Ag_3PO_4 with enhanced visible light activity. Chem Eng J 402:126183. https://doi.org/10.1016/j.cej.2020.126183

Lei J, Chen B, Zhou L, Ding N, Cai Z, Wang L, In S-I, Cui C, Zhou Y, Liu Y, Zhang J (2020) Efficient degradation of antibiotics in different water matrices through the photocatalysis of inverse Opal K-g-C_3N_4: insights into mechanism and assessment of antibacterial activity. Chem Eng J 400:125902. https://doi.org/10.1016/j.cej.2020.125902

Li Y, Bian Y, Qin H, Zhang Y, Bian Z (2017) Photocatalytic reduction behavior of hexavalent chromium on hydroxyl modified titanium dioxide. Appl Catal B 206:293–299. https://doi.org/10.1016/j.apcatb.2017.01.044

Li X, Shen R, Ma S, Chen X, Xie J (2018) Graphene-based heterojunction photocatalysts. Appl Surf Sci 430:53–107. https://doi.org/10.1016/j.apsusc.2017.08.194

Li B, Lai C, Zeng G, Huang D, Qin L, Zhang M, Cheng M, Liu X, Yi H, Zhou C, Huang F, Liu S, Fu Y (2019) Black phosphorus, a rising star 2D nanomaterial in the post-graphene era: synthesis, properties, modifications, and photocatalysis applications. Small 15(8):e1804565. https://doi.org/10.1002/smll.201804565

Liu L, Qi Y, Hu J, Liang Y, Cui W (2015) Efficient visible-light photocatalytic hydrogen evolution and enhanced photostability of core@shell Cu_2O@g-C_3N_4 octahedra. Appl Surf Sci 351:1146–1154. https://doi.org/10.1016/j.apsusc.2015.06.119

Liu H, Zhang Z, Meng J, Zhang J (2017) Novel visible-light-driven $CdIn_2S_4$/mesoporous g-C_3N_4 hybrids for efficient photocatalytic reduction of CO_2 to methanol. Mol Catal 430:9–19. https://doi.org/10.1016/j.molcata.2016.12.006

Liu Y, Yang S, Yin S-N, Feng L, Zang Y, Xue H (2018) In situ construction of fibrous AgNPs/g-C_3N_4 aerogel toward light-driven COx-free methanol dehydrogenation at room temperature. Chem Eng J 334:2401–2407. https://doi.org/10.1016/j.cej.2017.12.016

Liu Y, Xu C, Xie Y, Yang L, Ling Y, Chen L (2019) Au–Cu nanoalloy/TiO_2/MoS_2 ternary hybrid with enhanced photocatalytic hydrogen production. J Alloys Compds 820:153440. https://doi.org/10.1016/j.jallcom.2019.153440

Long Z, Li Q, Wei T, Zhang G, Ren Z (2020) Historical development and prospects of photocatalysts for pollutant removal in water. J Hazard Mater 395:122599. https://doi.org/10.1016/j.jhazmat.2020.122599

Lum PT, Foo KY, Zakaria NA, Palaniandy P (2019) Ash based nanocomposites for photocatalytic degradation of textile dye

pollutants: a review. Mater Chem Phys 241:122405. https://doi.org/10.1016/j.matchemphys.2019.122405

Luo X-L, He G-L, Fang Y-P, Xu Y-H (2018) Nickel sulfide/graphitic carbon nitride/strontium titanate (NiS/g-C_3N_4/$SrTiO_3$) composites with significantly enhanced photocatalytic hydrogen production activity. J Colloid Interface Sci 518:184–191. https://doi.org/10.1016/j.jcis.2018.02.038

Mahanthappa M, Kottam N, Yellappa S (2018) Enhanced Photocatalytic degradation of methylene blue dye using CuS-CdS nanocomposite under visible light irradiation. Appl Surf Sci 475:828–838. https://doi.org/10.1016/j.apsusc.2018.12.178

Makropoulou T, Kortidis I, Davididou K, Motaung DE, Chatzisymeon E (2020) Photocatalytic facile ZnO nanostructures for the elimination of the antibiotic sulfamethoxazole in water. J Water Process Eng 36:101299. https://doi.org/10.1016/j.jwpe.2020.101299

Mamba G, Gangashe G, Moss L, Hariganesh S, Thakur S, Vadivel S, Mishra AK, Vilakati GD, Muthuraj V, Nkambule TTI (2019) State of the art on the photocatalytic applications of graphene based nanostructures: from elimination of hazardous pollutants to disinfection and fuel generation. J Environ Chem Eng 8(2):103505. https://doi.org/10.1016/j.jece.2019.103505

Manea YK, Khan AM, Nabi SA (2019) Facile synthesis of Mesoporous Sm@ POA/TP and POA/TP nanocomposites with excellent performance for the photocatalytic degradation of MB and MG dyes. J Alloys Compd 791:1046–1062. https://doi.org/10.1016/j.jallcom.2019.03.091

Meng X, Zhang Z, Li X (2015) Synergetic photoelectrocatalytic reactors for environmental remediation: a review. J Photochem Photobiol, C 24:83–101. https://doi.org/10.1016/j.jphotochemrev.2015.07.003

Mishra M, Chun D-M (2015) α-Fe_2O_3 as a photocatalytic material: a review. Appl Catal A 498:126–141. https://doi.org/10.1016/j.apcata.2015.03.023

Mkhalid IA (2016) Photocatalytic degradation of herbicides under visible light using Pd–WO_3 nanorods. Ceram Int 42(14):15975–15980. https://doi.org/10.1016/j.ceramint.2016.07.100

Mohamed AS, AbuKhadra MR, Abdallah EA, El-Sherbeeny AM, Mahmoud RK (2020) The photocatalytic performance of silica fume based Co_3O_4/MCM-41 green nanocomposite for instantaneous degradation of Omethoate pesticide under visible light. J Photochem Photobiol, A 392:112434. https://doi.org/10.1016/j.jphotochem.2020.112434

Naffati N, Sampaio MJ, Da Silva ES, Nsib MF, Arfaoui Y, Houas A, Faria JL, Silva CG (2020) Carbon-nanotube/TiO_2 materials synthesized by a one-pot oxidation/hydrothermal route for the photocatalytic production of hydrogen from biomass derivatives. Mater Sci Semicond Process 115:105098. https://doi.org/10.1016/j.mssp.2020.105098

Nagajyothi PC, Devarayapalli KC, Shim J, Prabhakar Vattikuti SV (2020) Highly efficient white-LED-light-driven photocatalytic hydrogen production using highly crystalline $ZnFe_2O_4$/MoS_2 nanocomposites. Int J Hydrog Energy. https://doi.org/10.1016/j.ijhydene.2020.03.047

Neeraj G, Krishnan S, Kumar PS, Shriaishvarya KR, Kumar VV (2016) Performance study on sequestration of copper ions from contaminated water using newly synthesized high effective chitosan coated magnetic nanoparticles. J Mol Liq 214:335–346. https://doi.org/10.1016/j.molliq.2015.11.051

Nickheslat A, Amin MM, Izanloo H, Fatehizadeh A, Mousavi SM (2013) Phenol photocatalytic degradation by advanced oxidation process under ultraviolet radiation using titanium dioxide. J Environ Pub Health 2013:1–9. https://doi.org/10.1155/2013/815310

Nitoi I, Oancea P, Raileanu M, Crisan M, Constantin L, Cristea I (2015) UV–VIS photocatalytic degradation of nitrobenzene from water using heavy metal doped titania. J Ind Eng Chem 21:677–682. https://doi.org/10.1016/j.jiec.2014.03.036

Oliva J, Sanchez J, Servin SR, Ruiz-Santoyo JA, Garcia CR, Vallejo MA, Alvarez-Valteirra L, Gomez-Solis C (2020) Enhancing the photocatalytic degradation of ciprofloxacin contaminant using a combined laser irradiation (285/365 nm) and porous g-C_3N_4. Mater Chem Phys 252:123198. https://doi.org/10.1016/j.matchemphys.2020.123198

Olowoyo JO, Kumar M, Singh B, Oninla VO, Babalola JO, Valdés H, Vorontsov AV, Kumar U (2019) Self-assembled reduced graphene oxide-TiO_2 nanocomposites: synthesis, DFTB + calculations, and enhanced photocatalytic reduction of CO_2 to methanol. Carbon 147:385–397. https://doi.org/10.1016/j.carbon.2019.03.019

Qi YL, Han G, Song XC (2018) Enhanced photocatalytic degradation of phenol over Ag_3PO_4–$BiOCl_{1-x}$ Br x composites. Mater Res Bullet 102:16–23. https://doi.org/10.1016/j.materresbull.2018.02.019

Qu Y, Xu X, Huang R, Qi W, Su R, He Z (2019) Enhanced photocatalytic degradation of antibiotics in water over functionalized N, S-doped carbon quantum dots embedded ZnO nanoflowers under sunlight irradiation. Chem Eng J 382:123016. https://doi.org/10.1016/j.cej.2019.123016

Rakibuddin M, Kim H (2020) Samarium (III)-doped ZnO/graphitic – C_3N_4 composites for enhanced hydrogen generation from water under visible light photocatalysis. J. Alloys Compd 832:154887. https://doi.org/10.1016/j.jallcom.2020.154887

Ramos-Delgado NA, Hinojosa-Reyes L, Guzman-Mar IL, Gracia-Pinilla MA, Hernández-Ramírez A (2013) Synthesis by sol–gel of WO_3/TiO_2 for solar photocatalytic degradation of malathion pesticide. Catal Today 209:35–40. https://doi.org/10.1016/j.cattod.2012.11.011

Rani M, Shanker U (2018) Photocatalytic degradation of toxic phenols from water using bimetallic metal oxide nanostructures. Colloids Surf A 553:546–561. https://doi.org/10.1016/j.colsurfa.2018.05.071

Ren X, Zeng G, Tang L, Wang J, Wan J, Liu Y, Yu J, Yi H, Ye S, Deng R (2018) Sorption, transport and biodegradation—an insight into bioavailability of persistent organic pollutants in soil. Sci Total Environ 610:1154–1163. https://doi.org/10.1016/j.scitotenv.2017.08.089

Rodrigues J, Hatami T, Rosa JM, Basile Tambourgi E, Innocentini Mei LH (2019) Photocatalytic degradation using ZnO for the treatment of RB 19 and RB 21 dyes in industrial effluents and mathematical modeling of the process. Chem Eng Res Des 153:294–305. https://doi.org/10.1016/j.cherd.2019.10.021

Roslindawati H, Ramli M, Tuan ATA, Roshanida AR (2017) Overview on utilization of biodiesel by-product for biohydrogen production. J Clean Prod 172:314–324. https://doi.org/10.1016/j.jclepro.2017.10.160

Roushani M, Mavaei M, Rajabi HR (2015) Graphene quantum dots as novel and green nano-materials for the visible-light-driven photocatalytic degradation of cationic dye. J Mol Catal A 409:102–109. https://doi.org/10.1016/j.molcata.2015.08.011

Ruan X, Hu H, Che H, Che G, Li C, Liu C, Dong H (2018) Facile fabrication of Ag_2O/$Bi1_2GeO_{20}$ heterostructure with enhanced visible-light photocatalytic activity for the degradation of various antibiotics. J Alloys Compd 773:1089–1098. https://doi.org/10.1016/j.jallcom.2018.09.312

Saljooqi A, Shamspur T, Mostafavi A (2020) Synthesis of titanium nanoplate decorated by Pd and Fe_3O_4 nanoparticles immobilized on graphene oxide as a novel photocatalyst for degradation of parathion pesticide. Polyhedron 179:114371. https://doi.org/10.1016/j.poly.2020.114371

Samsudin MFR, Bacho N, Sufian S, Ng YH (2018) Photocatalytic degradation of phenol wastewater over Z-scheme g-C_3N_4/CNT/$BiVO_4$ heterostructure photocatalyst under solar light

irradiation. J Mol Liq 277:977–988. https://doi.org/10.1016/j.molliq.2018.10.160

Saravanan A, Karishma S, Jeevanantham S, Jeyasri S, Kiruthika AR, Kumar PS, Yaashikaa PR (2020) Optimization and modeling of reactive yellow adsorption by surface modified Delonix regia seed: study of nonlinear isotherm and kinetic parameters. Surf Interfaces 20:100520. https://doi.org/10.1016/j.surfin.2020.100520

Scott T, Zhao H, Deng W, Feng X, Li Y (2018) Photocatalytic degradation of phenol in water under simulated sunlight by an ultrathin MgO coated Ag/TiO_2 nanocomposite. Chemosphere 216:1–8. https://doi.org/10.1016/j.chemosphere.2018.10.083

Shaban YA, El Sayed MA, El Maradny AA, Al Farawati RK, Al Zobidi MI (2013) Photocatalytic degradation of phenol in natural seawater using visible light active carbon modified (CM)-n-TiO_2 nanoparticles under UV light and natural sunlight illuminations. Chemosphere 91:307–313. https://doi.org/10.1016/j.chemosphere.2012.11.035

Shahidi D, Roy R, Azzouz A (2015) Advances in catalytic oxidation of organic pollutants—prospects for thorough mineralization by natural clay catalysts. Appl Catal B 174–175:277–292. https://doi.org/10.1016/j.apcatb.2015.02.042

Shahzad K, Tahir MB, Sagir M (2019a) Engineering the performance of heterogeneous WO_3/fullerene@Ni_3B/$Ni(OH)_2$ Photocatalysts for Hydrogen Generation. Int J Hydrog Energy 44:21738–21745. https://doi.org/10.1016/j.ijhydene.2019.06.148

Shahzad K, Tahir MB, Sagir M, Kabili MR (2019b) Role of $CuCo_2S_4$ in Z-scheme $MoSe_2$/$BiVO_4$ composite for efficient photocatalytic reduction of heavy metals. Ceram Int 45:23225–23232. https://doi.org/10.1016/j.ceramint.2019.08.018

Sharma A, Lee B-K (2017) Photocatalytic reduction of carbon dioxide to methanol using nickel-loaded TiO_2 supported on activated carbon fiber. Catal Today 298:158–167. https://doi.org/10.1016/j.cattod.2017.05.003

Shet A, Vidya SK (2016) Solar light mediated photocatalytic degradation of phenol using Ag core—TiO_2 shell (Ag@TiO_2) nanoparticles in batch and fluidized bed reactor. Sol Energy 127:67–78. https://doi.org/10.1016/j.solener.2015.12.049

Shibin OM, Yesodharan S, Yesodharan EP (2015) Sunlight induced photocatalytic degradation of herbicide diquat in water in presence of ZnO. J Environ Chem Eng 3(2):1107–1116. https://doi.org/10.1016/j.jece.2015.04.026

Shwetharani R, Balakrishna RG (2016) Efficient algal lipid extraction via photocatalysis and its conversion to biofuel. Appl Energy 168:364–374. https://doi.org/10.1016/j.apenergy.2016.01.087

Singh S, Mahalingam H, Singh PK (2013) Polymer-supported titanium dioxide photocatalysts for environmental remediation: a review. Appl Catal A-Gen 462–463:178–195. https://doi.org/10.1016/j.apcata.2013.04.039

Sobahi T (2017) Photocatalytic degradation of herbicides under visible light using Ni-Pr_2O_3 nanocomposites. J Alloys Compds 695:1279–1284. https://doi.org/10.1016/j.jallcom.2016.10.257

Soliman AM, Elsuccary SAA, Ali IM, Ayesh AI (2017) Photocatalytic activity of transition metal ions-loaded activated carbon: degradation of crystal violet dye under solar radiation. J Water Process Eng 17:245–255. https://doi.org/10.1016/j.jwpe.2017.04.010

Sood S, Kumar S, Umar A, Kaur A, Mehta SK, Kansal SK (2015) TiO_2 quantum dots for the photocatalytic degradation of indigo carmine dye. J Alloys Compd 650:193–198. https://doi.org/10.1016/j.jallcom.2015.07.164

Sun X, Lu J, Wu J, Guan D, Liu Q, Yan N (2019) Enhancing photocatalytic activity on gas-phase heavy metal oxidation with self-assembled BiOI/BiOCl microflowers. J Colloid Interface Sci 546:32–42. https://doi.org/10.1016/j.jcis.2019.03.049

Sun F, Qi H, Xie Y, Ma Q, He W, Xu D, Wang G, Yu W, Wang T, Dong X (2020a) Flexible self-supporting bifunctional [TiO_2/C]//[Bi_2WO_6/C] carbon-based Janus nanofiber heterojunction photocatalysts for efficient hydrogen evolution and degradation of organic pollutant. J Alloys Compd 830:154673. https://doi.org/10.1016/j.jallcom.2020.154673

Sun K, Zhao X, Zhang Y, Wu D, Zhou X, Xie F, Tang Z, Wang X (2020b) Enhanced photocarrier separation in novel Z-scheme Cu_2ZnSnS_4/Cu_2O heterojunction for excellent photocatalyst hydrogen generation. Mater Chem Phys 251:123172. https://doi.org/10.1016/j.matchemphys.2020.123172

Tamilarasan K, Banu R, Kumar D, Park JH (2019) Influence of mild-ozone assisted disperser pretreatment on the enhanced biogas generation and biodegradability of green marine macroalgae. Front Energ Res 7:89. https://doi.org/10.3389/fenrg.2019.00089

Tran VA, Kadam AN, Lee S-W (2020) Adsorption-assisted photocatalytic degradation of methyl orange dye by zeolite-imidazole-framework-derived nanoparticles. J Alloys Compds 835:155414. https://doi.org/10.1016/j.jallcom.2020.155414

Vaiano V, Lara MA, Iervolino G, Matarangolo M, Navio JA, Hidalgo MC (2018) Photocatalytic H_2 production from glycerol aqueous solutions over fluorinated Pt–TiO_2 with high 001 facet exposure. J Photochem Photobiol, A 365:52–59. https://doi.org/10.1016/j.jphotochem.2018.07.032

Wang W, Zhang J, Wang H, Chen L, Bian Z (2016) Photocatalytic and electrocatalytic reduction of CO_2 to methanol by the homogeneous pyridine-based systems. Appl Catal A 520:1–6. https://doi.org/10.1016/j.apcata.2016.04.003

Wang D, Wang X, Liu J, Zhang M, Song Y, Zhang Z, Wang J (2020) Preparation of high proportion of Z-scheme Er_{3+}:$Y_3Al_5O1_2$@Nb_2O_5/Pt/In_2O_3 composite for enhanced visible-light driven photocatalytic hydrogen production. Mater Sci Eng, B 257:114549. https://doi.org/10.1016/j.mseb.2020.114549

Wen J, Li X, Li H, Ma S, He K, Xu Y, Fang Y, Liu W, Gao Q (2015) Enhanced visible-light H_2 evolution of g-C_3N_4 photocatalysts via the synergetic effect of amorphous NiS and cheap metal-free carbon black nanoparticles as co-catalysts. Appl Surf Sci 358:204–212. https://doi.org/10.1016/j.apsusc.2015.08.244

Wong CL, Tan YN, Mohamed AR (2011) Photocatalytic degradation of phenol using immobilized TiO_2 nanotube photocatalysts. J Nanotechnol 2011:1–9. https://doi.org/10.1155/2011/904629

Wood D, Shaw S, Cawte T, Shanen E, Van Heyst B (2019) An overview of photocatalyst immobilization methods for air pollution remediation. Chem Eng J 391:123490. https://doi.org/10.1016/j.cej.2019.123490

Xiao Y, Guo X, Liu J, Liu L, Zhang F, Li C (2019) Development of a bismuth-based metal-organic framework for photocatalytic hydrogen production. Chin J Catal 40:1339–1344. https://doi.org/10.1016/s1872-2067(19)63329-2

Xie W-J, Li X, Zhang F-J (2020) Mo-vacancy induced high performance for photocatalytic hydrogen production over MoS_2 nanosheets cocatalyst. Chem Phys Lett 746:137276. https://doi.org/10.1016/j.cplett.2020.137276

Xing X, Tang S, Hong H, Jin H (2020) Concentrated solar photocatalysis for hydrogen generation from water by titania-containing gold nanoparticles. Int J Hydrog Energy 45(16):9612–9623. https://doi.org/10.1016/j.ijhydene.2020.01.197

Xu J, Li X, Niu J, Chen M, Yue J (2020) Synthesis of direct Z-Scheme Bi_3TaO_7/CdS composite photocatalysts with enhanced photocatalytic performance for ciprofloxacin degradation under visible light irradiation. J Alloys Compds 834:155061. https://doi.org/10.1016/j.jallcom.2020.155061

Yadav R, Amoli V, Singh J, Tripathi MK, Bhanja P, Bhaumik A, Sinha AK (2018) Plasmonic gold deposited on mesoporous $Ti_xSi_{1-x}O_2$ with isolated silica in lattice: an excellent photocatalyst for photocatalytic conversion of CO_2 into methanol under visible light irradiation. J CO2 Util 27:11–21. https://doi.org/10.1016/j.jcou.2018.06.016

Yang G, Wang J (2019) Ultrasound combined with dilute acid pretreatment of grass for improvement of fermentative hydrogen production. Bioresour Technol 275:10–18. https://doi.org/10.1016/j.biortech.2018.12.013

Yang J, Sun X, Wang R, Zhu M, Yang W, Huang H, Shi W (2020) An Au-nanoparticle decorated $Sr_{0.76}Ce_{0.16}WO_4$ photocatalyst for H_2 evolution under visible-light irradiation. Int J Hydrog Energy 45(23):12702–12710. https://doi.org/10.1016/j.ijhydene.2020.02.208

Yin H, Cao Y, Fan T, Qiu B, Zhang M, Yao J, Li P, Liu X, Chen S (2020) Construction of carbon bridged TiO_2/CdS tandem Z-scheme heterojunctions toward efficient photocatalytic antibiotic degradation and Cr(VI) reduction. J Alloys Compd 824:153915. https://doi.org/10.1016/j.jallcom.2020.153915

Younis SA, Kwon EE, Qasim M, Kim K-H, Kim T, Kukkar D, Dou X, Ali I (2020) Metal-organic framework as a photocatalyst: progress in modulation strategies and environmental/energy applications. Prog Energy Combust Sci 81:100870. https://doi.org/10.1016/j.pecs.2020.100870

Yu J, Chen Z, Zeng L, Ma Y, Feng Z, Wu Y, Lin H, Zhao L, He Y (2018) Synthesis of carbon-doped $KNbO_3$ photocatalyst with excellent performance for photocatalytic hydrogen production. Sol Energy Mater Sol Cells 179:45–56. https://doi.org/10.1016/j.solmat.2018.01.043

Yu X, Zhao J, Huang J, Zhao J, Guo Y, Tang Y, Ma X, Li Z, Guo Q, Zhao J (2020) Visible light photocatalysis of amorphous Cl-Ta_2O_{5-x} microspheres for stabilized hydrogen generation. J Colloid Interface Sci 572:141–150. https://doi.org/10.1016/j.jcis.2020.03.030

Yuqing H, Qiaoying L, Shenyuan B, Yufeng L, Zhipeng G, Jinlong Z, Baozhu T (2020) Z-scheme heterostructure BiOCl–Ag–AgBr with enhanced sunlight-driven photocatalytic activity in simultaneous removal of Cr_{6+} and phenol contaminants. Catal Today. https://doi.org/10.1016/j.cattod.2020.06.054

Zahedi F, Behpour M, Ghoreishi SM, Khalilian H (2015) Photocatalytic degradation of paraquat herbicide in the presence TiO_2 nanostructure thin films under visible and sun light irradiation using continuous flow photoreactor. Sol Energy 120:287–295. https://doi.org/10.1016/j.solener.2015.07.010

Zhang W, Xiao X, Zheng L, Wan C (2015) Fabrication of TiO_2/MoS_2@zeolite photocatalyst and its photocatalytic activity for degradation of methyl orange under visible light. Appl Surf Sci 358:468–478. https://doi.org/10.1016/j.apsusc.2015.08.054

Zhang F-J, Li X, Sun X-Y, Kong C, Xie W-J, Li Z, Liu J (2019a) Surface partially oxidized MoS_2 nanosheets as a higher efficient cocatalyst for photocatalytic hydrogen production. Appl Surf Sci 487:734–742. https://doi.org/10.1016/j.apsusc.2019.04.258

Zhang J, Wang H, Yuan X, Zeng G, Tu W, Wang S (2019b) Tailored indium sulfide-based materials for solar-energy conversion and utilization. J Photochem Photobiol, C 38:1–26. https://doi.org/10.1016/j.jphotochemrev.2018.11.001

Zhang Q, Wang M, Ao M, Luo Y, Zhang A, Zhao L, Yan L, Deng F, Luo X (2019c) Solvothermal synthesis of Z-scheme $AgIn_5S_8$/Bi_2WO_6 nano-heterojunction with excellent performance for photocatalytic degradation and Cr(VI) reduction. J Alloys Compd 805:41–49. https://doi.org/10.1016/j.jallcom.2019.06.331

Zhang Q, Jiang L, Wang J, Zhu Y, Pu Y, Dai W (2020) Photocatalytic degradation of tetracycline antibiotics using three-dimensional network structure perylene diimide supramolecular organic photocatalyst under visible-light irradiation. Appl Catal B 277:119122. https://doi.org/10.1016/j.apcatb.2020.119122

Zhao Y, Wang Y, Xiao G, Su H (2019) Fabrication of biomaterial/TiO_2 composite photocatalysts for the selective removal of trace environmental pollutants. Chin J Chem Eng 27(6):1416–1428. https://doi.org/10.1016/j.cjche.2019.02.003

Zhao X, Xie W, Deng Z, Wang G, Cao A, Chen H, Yang B, Wang Z, Su X, Yang C (2020) Salt templated synthesis of NiO/TiO_2 supported carbon nanosheets for photocatalytic hydrogen production. Colloids Surf A 587:124365. https://doi.org/10.1016/j.colsurfa.2019.124365

Zhu L, Gu W, Li H, Zou W, Liu H, Zhang Y, Wu Q, Fu Z, Lu Y (2020) Enhancing the photocatalytic hydrogen production performance of $SrTiO_3$ by coating with a hydrophilic poloxamer. Appl Surf Sci 528:146837. https://doi.org/10.1016/j.apsusc.2020.146837

Publisher's Note Springer Nature remains neutral with regard to jurisdictional claims in published maps and institutional affiliations.